The Taos Plateau and the Rio Grande Gorge - First-day road log from Taos to Questa, the Wild Rivers Recreation Area, Arroyo Hondo, the Dunn Bridge, the Rio Grande Gorge Bridge, and return to Taos

Adam S. Read, Paul W. Bauer, Ren A. Thompson, Keith I. Kelson, and William R. Muehlberger

2004, pp. 1-36. https://doi.org/10.56577/FFC-55.1

in:

Geology of the Taos Region, Brister, Brian; Bauer, Paul W.; Read, Adam S.; Lueth, Virgil W.; [eds.], New Mexico Geological Society 55 th Annual Fall Field Conference Guidebook, 440 p. https://doi.org/10.56577/FFC-55

This page is intentionally left blank to maintain order of facing pages.

THE TAOS PLATEAU AND RIO GRANDE GORGE

FIRST-DAY ROAD LOG FROM TAOS TO QUESTA, THE WILD RIVERS RECREATION AREA, ARROYO HONDO, THE DUNN BRIDGE, THE RIO GRANDE GORGE BRIDGE, AND RETURN TO TAOS

ADAM S. READ, PAUL W. BAUER, REN A. THOMPSON, KEITH I. KELSON,
AND WILLIAM R. MUEHLBERGER

Assembly Point: Sagebrush Inn, Taos

Departure Time: 7:30 AM

Distance: 107.2 miles

Six stops plus two optional stops

SUMMARY

The first day of the conference will focus on the volcanic rocks of the Taos Plateau volcanic field and the temporal and geographic relationships between volcanism, sedimentation in the San Luis Basin of the Rio Grande rift, and the fluvial / tectonic geomorphology of the Rio Grande and its tributaries. We will work downstream along the Rio Grande gorge, from above the Red River confluence in the Wild Rivers Recreation Area near Questa to below the Gorge Bridge near Taos. The rim of the gorge provides spectacular views of the geologic features exposed in the gorge walls, the volcanoes on the plateau, and the uplifts around the edges of the rift basin. If you neglect to bring a camera, you will regret it, as this is some of the most dramatic scenery in New Mexico. *Note that GPS waypoints [in brackets] have been added to the roadlogs this year at turns and stops to facilitate navigation (see Appendix at the end of the roadlogs).* We have posted these coordinates on the NMGS website <geo-info.nmt.edu/nmgs/fieldtrip/2004> if you would like to upload them to your GPS unit. Relative bearings to points of interest in several log entries utilize the clock system; relative to vehicle orientation, 12:00 is directly ahead, 3:00 is to the right and so forth. The eleven color plates following the road logs are referred to throughout the road logs and in several of the papers.

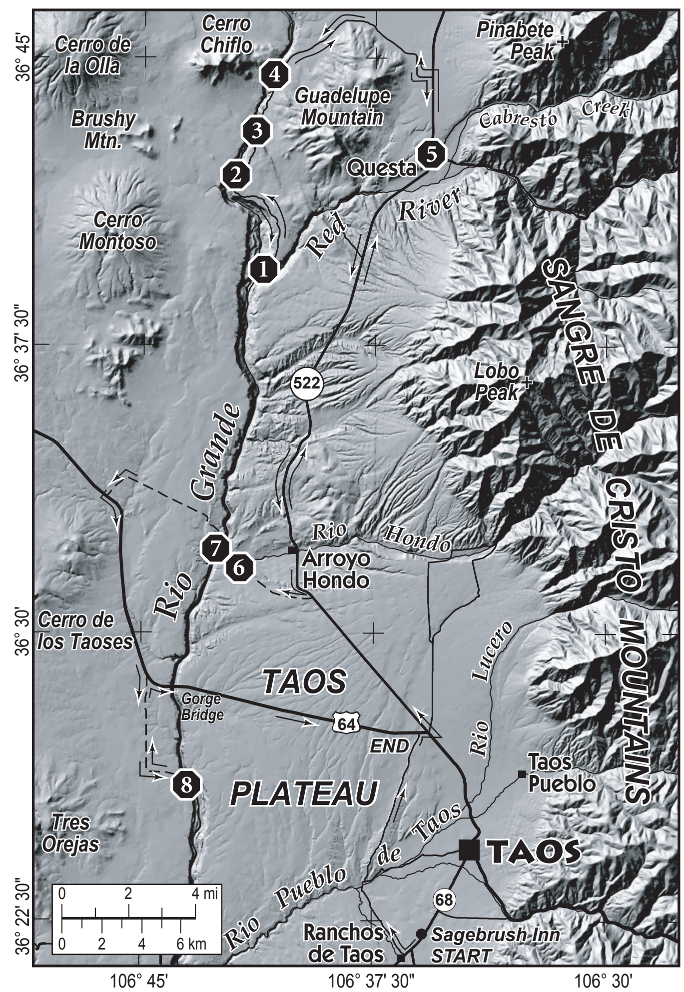

0.0 [1] Depart from the southwest entrance of the Sagebrush Inn. Turn right on NM-68.

The Sagebrush Inn, a mission-style adobe structure built in 1929 contains many works of southwestern art including Native American pottery, artifacts, paintings, Navajo rugs, and Spanish colonial antiques. For a time, Georgia O'Keefe lived and painted here.

We are driving on a moderately dissected late Pleistocene alluvial fan complex derived from the Sangre de Cristo Mountains to the south. The source rocks for these fan deposits are Pennsylvanian sedimentary rocks, primarily sandstone, shale and minor limestone. The southern Sangre de Cristo fault lies along the prominent break in slope to the east; this fault is the principal west-down normal fault along the eastern margin of the northern Rio Grande rift in the Taos area. **0.0**

0.5 On left is the junction with NM-518 to Talpa. **Continue straight** into the Village of Ranchos de Taos. We are descending into the north-trending valley of the Rio Grande del Rancho, a perennial tributary of the Rio Pueblo de Taos that drains the Picuris and Sangre de Cristo Mountains to the south. This valley contains several broad fluvial terraces associated with coarse alluvial gravel. **0.5**

0.8 **Turn right onto NM-240 at the bottom of the grade**
[2] (if you pass the St. Francis de Assisi church, you've gone too far) towards Los Cordovas, Ranchitos, and the Martinez Hacienda. The Hacienda, built in 1804, is one of the finest surviving examples of Spanish Colonial architecture, and is now a museum open to the public. **0.3**

1.1 We are driving along the Qt4 terrace of the Rio Grande del Rancho valley, which is associated with a poorly sorted gravel consisting almost exclusively of Pennsylvanian sandstone pebbles and cobbles. Clast imbrications suggest a northwesterly flow direction. Soils formed on this terrace have stage III calcium carbonate accumulation and argillic B horizons, suggesting a late Pleistocene age (Kelson, 1986; Bauer et al., 1999b). This gravel is deposited on older, semi-consolidated, basin-fill deposits ("Blueberry Hill deposits" of Bauer and Kelson, 2001) and clast imbrications in this area suggest northwesterly paleoflow directions. **0.3**

2.1 We are driving down the terrace riser between the Qt4 terrace and the inset Qt6 terrace of Kelson (1986), which has been generalized as terrace Qty by Bauer et al. (1999b) and Kelson and Bauer (2003). The soils formed on this terrace have stage I calcium carbonate accumulation, and are interpreted to be latest Pleistocene to early Holocene in age (Bauer et al., 1999b; Kelson and Bauer, 2003). These terraces merge with correlative terraces flanking the Rio Pueblo de Taos, which flows from east to west just ahead. **1.0**

3.1 **Bear right, just after sharp left bend, staying on**
[3] **NM-240.** Note Pliocene basalt exposed on northern side of Rio Pueblo de Taos valley. This basalt borders both sides of the southern end of the Arroyo Seco valley, which is a tributary that enters the Rio Pueblo de Taos directly downstream of NM-240. **1.0**

3.2 Crossing the Rio Pueblo de Taos, the largest stream draining the eastern side of the Taos Plateau. At this road crossing, the thin valley-floor alluvium overlies Pliocene basalt, and consists of a mixed population of clasts from tributaries draining Pennsylvanian sedimentary rocks and crystalline metamorphic clasts from tributaries draining Precambrian rocks. Kelson and Wells (1989) have shown that the tributaries draining sedimentary rocks, compared to those draining metamorphic rocks, have relatively low unit discharge, low bankfull discharge, and short-duration discharge peaks. The source-area lithologies of the tributaries draining the Sangre de Cristo Mountains control the present-day hydrology of the channels, and thus strongly influence stream power and bedload transport along the Rio Pueblo de Taos (Kelson and Wells, 1987, 1989). The development of the Rio Pueblo de Taos valley over the late Quaternary is a function of these lithologic controls on fluvial hydrology over geologic time (Kelson, 1986). **0.1**

3.4 **Turn left onto Blueberry Hill Road.** Named after the
[4] Fats Domino song by truant high school students (Julyan, 1996). **0.2**

3.5 As we ascend out of the Rio Pueblo de Taos valley (see Fig. 1.1), we are driving up through the "Blueberry Hill deposits" of Kelson and Bauer (2003), which consist primarily of sand and pebbles derived from a south-flowing ancestral Rio Grande as well as ancestral tributary alluvial fans. These distinct, semi-consolidated deposits are commonly crossbedded, characteristically oxidized to yellowish-orange colors, and typically stained with black oxide coatings. Granitic, metamorphic, and basaltic clasts, as well as rare sandstone clasts, suggest local sources. Despite the proximal provenance, clasts from this deposit are all deeply weathered attesting to their long interaction with groundwater. Kelson (1986) referred to these deposits as "Basin Fill deposits," and interpreted them as middle Pleistocene in age. **0.1**

3.8 Roadcut on left exposes Qf1 gravels that unconform ably overlie the "Blueberry Hill deposits." This overlying gravel contains mostly granitic clasts, quartzite and other metamorphic clasts, and is associated with a large, southwesterly sloping alluvial fan (map unit Qf1; Kelson and Bauer, 2003) from the ancestral Rio Lucero, Arroyo Seco, and Rio Hondo drainage basins northeast of the Town of Taos. At this locality, the Qf1 alluvial-fan deposits are thin (less than 2 m), but the deposit thickens to several tens-of-meters in a northeasterly direction toward the Sangre de Cristo Mountains. Soils associated with these deposits are generally eroded remnants of well-developed soils with stage IV calcium carbonate accumulation. Kelson (1986) correlated these deposits with those containing an ash dated at 1.27 ± 0.02 Ma using ^{40}Ar/^{39}Ar methods (Bauer et al., 1999a; Bauer and Kelson, 1997). **0.3**

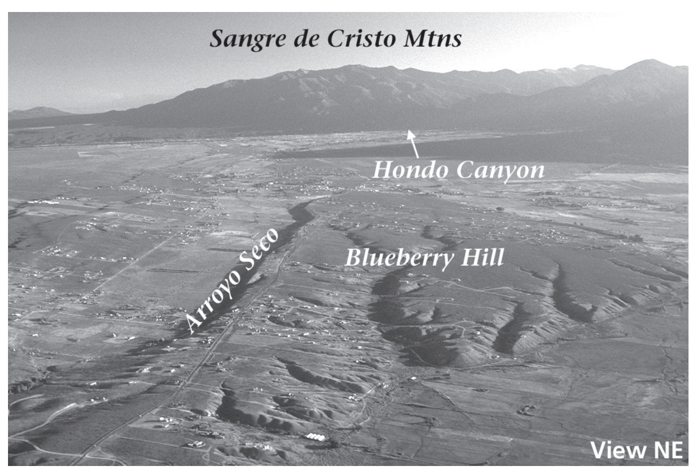

FIGURE 1.1. Aerial view northeastward of Blueberry Hill with the Sangre de Cristo Mountains in the distance. Blueberry Hill is an erosional remnant of the Tertiary/Quaternary Blueberry Hill basin fill deposit (QTbh) capped by a Pleistocene alluvial fan gravel (Qf1). The surrounding land is composed of younger alluvial fans derived from Arroyo Hondo and adjacent canyons in the Sangre de Cristo Mountains. Arroyo Seco is a strongly asymmetrical drainage that is slowly eroding the west edge of Blueberry Hill. Boreholes and geophysical data suggest that a complex zone of intrabasinal normal faults exists in the subsurface between Blueberry Hill and the mountain front.

5.3 KTAO radio station on left, touted as the "World's Most Powerful Solar Radio Station," on your FM dial at 101.9, utilizes a photovoltaic-powered transmitter atop Picuris Peak that transmits a signal of up to 50,000 watts that can be received by listeners within a 40-mile radius. **1.5**

6.8 Excellent view of the asymmetric profile of the Arroyo Seco drainage on left (see sidebar 1.1 later in this log). This valley contains three broad fluvial terraces inset into the "Blueberry Hill deposits" and the Qf1 alluvial-fan deposits (Bauer and Kelson, 2001), both preserved along the western flank of the valley. At this point, the latest Pleistocene Qty terrace is 2 m above the valley floor, the late Pleistocene Qt4 terrace is 6 m above the valley floor, and the middle(?) Pleistocene Qt2 terrace is 12 m above the valley floor (Kelson, 1986; Bauer and Kelson, 2001), although the terrace long-profiles diverge downstream. These terraces are continuous with correlative surfaces along the Rio Pueblo de Taos and Rio Grande del Rancho to the south. These terraces likely reflect the response of the Arroyo Seco tributary to base-level fall imposed by incision along the main-stem Rio Pueblo de Taos, which in turn was influenced by base-level fall along the Rio Grande as well as by climate change (Kelson, 1986). The response of this fluvial system to these external factors was influenced by discharge characteristics and source-area lithologies (Kelson and Wells, 1987, 1989; Kelson, 1986). **1.5**

6.9 Small quarry in Qf1 gravel is visible on right. This deposit is used extensively for building material locally. **0.1**

7.3 Eototo Rd. on the right leads to the Millicent Rogers Museum. The museum opened in 1956 to display the collection of southwestern art owned by Millicent Rogers, granddaughter of Henry Huttleston Rogers**,** an original founder of Standard Oil. The museum continues to add to this collection of northern New Mexico cultural artifacts by local Hispanic and native artists and craftsmen. **0.4**

7.5 Directly ahead in distance is Hondo Canyon, one of the sources of the extensive alluvial-fan deposits that extend as far west as Blueberry Hill. The Rio Hondo and its tributaries are eroding crystalline granitic and metamorphic rocks. Present-day hydrologic data from this basin show that it produces relatively high unit discharge (i.e., water volume per unit area), and that the discharge peaks are larger and longer-lasting than those produced by nearby basins underlain by sedimentary rocks. **0.2**

7.9 Ahead at 12:00 are the massive cliffs on the south side of Lucero Peak (also called El Salto locally). The 10,831 ft (3301 m) peak exposes part of the 22-23 Ma Lucero Peak pluton that is related to the Questa Caldera (Lipman and Reed, 1989). Wheeler Peak, the highest point in New Mexico at 13,161 feet (4011 meters), is visible on the skyline at 1:00 and is composed of Proterozoic layered gneiss (Lipman and Reed, 1989). **0.4**

8.2 **Turn right at intersection with US-64**. US-64 West
[5] leads across the basin to the Gorge Bridge and on to Tres Piedras ("three rocks"). **0.3**

8.4 **Turn left onto NM-522 north at light**. This light was
[6] formerly known as the "Blinking Light" (this was one of only two traffic lights in Taos some 20 years ago). NM-150 to the right leads to the village of Arroyo Seco ("dry wash," a rather common New Mexico placename), and then follows Hondo Canyon into the mountains to the Taos Ski Valley. The Ski Valley occupies the former copper and gold mining camp of Twining. Pueblo Peak is the high peak visible at 3:00, and Wheeler Peak is visible at 12:00 on skyline. **0.2**

8.5 Sand and gravel operation on the left. The highway descends into an abandoned valley filled with latest Pleistocene to early Holocene alluvial-fan deposits. This valley may have been an earlier course of the Rio Lucero, one of the primary sources of alluvial-fan deposits on the Sangre de Cristo Mountains piedmont. **0.1**

8.6 About a mile east of here is the 810-ft-deep Taos Pueblo Acequia Well (BIA-12). A detailed lithology log of well cuttings was recently completed by Jackson-Paul et al., 2002. Interpreted stratigraphic intervals are: 0-60 ft–no sample available; 60-260 ft–piedmont deposits, consisting of upward fining sequences of fine to coarse sand and pebble gravel; 260-810 ft–Quaternary/Tertiary basin-fill deposits, including the Blueberry Hill deposit. **0.1**

10.6 Just to the west is the 1000-ft-deep Taos Pueblo Tract B Well (BIA-7). According to the detailed lithology logging by Jackson-Paul et al. (2002) of the NMBGMR, from 0 - 600 ft the well penetrated pebbly sand containing clasts of quartzite, sandstone, granite, schist, and gneiss interpreted as Quaternary/Tertiary alluvial deposits derived from the Sangre de Cristo Mountains; 600-850 ft of intermediate volcanic rock interpreted as Pliocene Servilleta Basalt; and 850-1000 ft of pebbly sand with gravel clasts of basalt, quartzite, sandstone, granite, and schist interpreted as Santa Fe Group basin fill. **2.0**

10.9 Hondo Canyon is visible at 3:00. We are now at the axis of the Gorge arch (see sidebar 1.1). We are driving north across the Qf1 alluvial fan, which is associated with coarse gravel derived from the headwaters of Rio Hondo and Arroyo Seco. The Hondo fan exhibits many characteristics typical of fans in semi-arid environments like the Taos region. The fan is convex along the transect of highway NM-522, with the topographically high fan axis located at the Taos Municipal Airport. The down-fan gradient is fairly steep at the mountain front, and is gradually shallower to the southwest. In addition, the fan is dissected by arroyos that drain obliquely away from the fan axis, as related to the convex shape of the fan.

Over the next several miles, we cross over a northeast-trending drainage divide on the high Qf1 alluvial fan that separates domains with opposite drainage asymmetries (see sidebar 1.1).

SIDEBAR 1.1 - The Gorge arch and asymmetric drainages of the Taos area.

Muehlberger (1979), Peterson (1981) and Dungan et al. (1984) noted that asymmetric arroyos northwest of the Hondo fan axis have steeper valley walls on their northern sides, whereas arroyos southeast of the fan axis have steeper valley walls on their southern sides. From these relations, they interpreted the presence of a broad tectonic uplift they named the "Gorge Arch."

A recent, unpublished air photo analysis by Elsbeth Atencio of the symmetry of drainages in the region has confirmed the original patterns observed by Peterson (1981). However, Atencio identified more asymmetrical drainages in her study, and she also marked drainages that are symmetrical. Her map patterns are shown on Figure 1.2. Note that south of the Gorge arch (the Taos airport is built on the arch axis), streams have steeper cut-banks on their sides nearest the Sangre de Cristo fault to the southeast. This drainage-asymmetry domain south of the Gorge arch could be explained by differential rotation of a single hanging-wall block along the Sangre de Cristo fault that has a structural hinge along the axis of the Gorge arch. Along the mapped Los Cordovas faults, perhaps drainage asymmetries are better explained by domino-style rotation of smaller blocks. Note that domains of symmetrical drainages exist south of Taos, along the Rio Pueblo de Taos, and along the Rio Grande gorge where the Qf1 and QTbh have been eroded.

Throughout these roadlogs, we draw attention to the interesting changes in the patterns of the asymmetric drainages on the eastern Taos Plateau. Although we are not necessarily advocating a tectonic origin, we chose to use the term 'tilted' to indicate drainage-asymmetry vergence because non-genetic descriptions of stream-asymmetry morphology are cumbersome. For instance, the asymmetric drainages described above with steeper southeast sides south of the Gorge arch will be called 'southeast-tilted'.

In addition, we are driving across the northern projections of the Los Cordovas faults, which are a series of normal faults as much as 12 km long that displace Tertiary basalt (Lambert, 1966). Machette and Personius (1984) reported that early Pleistocene deposits are displaced along the faults, and that the most recent movement is middle Pleistocene. **0.3**

11.6 Several of the volcanoes of the Taos Plateau volcanic field are visible from this vantage point (Fig. 1.3). Ahead, at 12:00, in the far distance is San Antonio Mountain, 10 km south of the Colorado border. San Antonio Mountain is a striking example of a 3 Ma monolithologic dacite shield volcano superimposed on an older andesitic eruptive center. The low hills in the foreground include the 4 Ma rhyolite of No Agua Peaks ("no water") and other small basaltic-andesite and basalt shields of the Taos Plateau. At 12:30, the low shield in the distance is Cerro de la Olla ("pot-shaped mountain"), immediately in front of that volcano is Cerro Montoso ("brushy or wooded mountain"), and in the densely vegetated hill slopes at 11:00 are the Cerro de los Taoses volcanoes. All three centers are olivine-andesite volcanoes and range in age from 5.8 Ma to 4.8 Ma. **0.7**

12.1 Highway crosses a north-tilted asymmetric valley. We are now on the north-tilted domain of drainage asymmetries, and have crossed the Gorge arch. Lobo Peak, visible at 2:30, is composed of Paleoproterozoic quartzite and felsic gneiss. **0.5**

13.0 Highway crosses a deeply incised, north-tilted asymmetric valley. **0.9**

13.6 Just as the highway begins descent into the Arroyo Hondo drainage is a dirt road (B-007) on left that leads to Dunn's Bridge across the Rio Grande; the route we will take for several stops when we return from Questa. **0.6**

13.9 As we descend into Arroyo Hondo, the highway road cut exposes the Qf1 alluvial-fan gravel, which unconformably overlies the "Basin Fill deposits" of Kelson (1986). At the base of this hill (locally known as "Hondo Hill"), we are driving across the latest Pleistocene Qt6 surface of Kelson (1986), and then we descend onto the Holocene Qt7 terrace and the active floodplain of Rio Hondo. Based on measurements of bankfull channel geometry, channel gradient, and bed-material grain sizes, this channel has high bedload shear stress relative to channels within the Rio Pueblo de Taos drainage system. Rio Hondo has higher bedload transport rates and larger bedload particle sizes than Rio Pueblo de Taos, which has influenced its long-term adjustment to incision along the master Rio Grande channel. **0.3**

14.4 Mile marker 6. The ca. 5 Ma Cerro Negro dacite shield volcano is visible at 1:30 sticking up through onlapping alluvial fan deposits. The dacite characteristically contains two pyroxenes, has dark glassy groundmass, has few or no plagioclase phenocrysts, and coarse orthopyroxene phenocrysts contain resorbed olivine. **0.5**

15.1 Village of Arroyo Hondo ("deep canyon"). This valley contains a well-preserved sequence of six fluvial terraces inset into basin fill sediments interlayered with flows of Servilleta Basalt (as redefined by Lipman and Mehnert, 1979) and Cerro Negro dacite (Kelson, 1986; Kelson and Wells, 1987).

The village was established as a land grant in 1815. Simeon Turley, who settled in 1830, built a water-powered mill here. He later built a distillery and employed many locals in both enterprises. Following the scalping and murder of Governor Carlos Bent in Taos in 1847, a mob, angry about Anglo rule following the Mexican-American war, stormed the mill and eventually murdered Turley to seize the property (Bullock, 1973). **0.7**

15.2 Crossing over the Rio Hondo. The roadcut on the eastern side of the highway exposes a prominent paleochannel filled with coarse gravel that is typical of latest Pleistocene deposits along the Rio Hondo. Just ahead, on the east side of the road, is a roadcut exposure that represents outflow of the 5.7 Ma Cerro Negro rhyodacite volcano. Like other

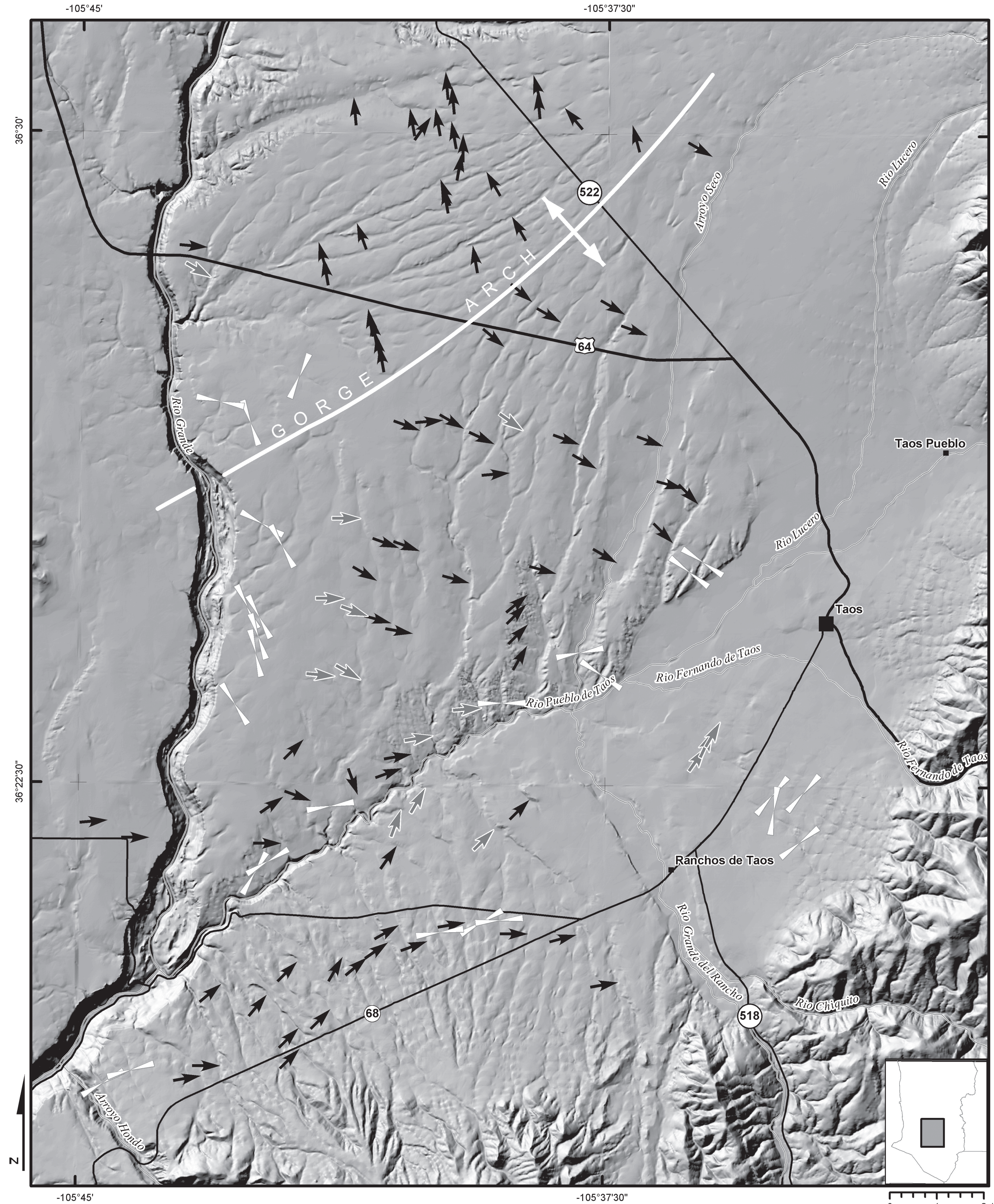

FIGURE 1.2. Digital Elevation Model (DEM) image of the Taos Valley showing stream profile asymmetries (black arrows, and gray arrows with less confidence, point to steep side of drainage) and symmetrical stream profiles (white arrows indicate that drainage has no discernable asymmetry). These data are from a 2003 stereographic air photo analysis of the region by Elsbeth Atencio using USGS 1997 1:40,000 NAPP air photos.

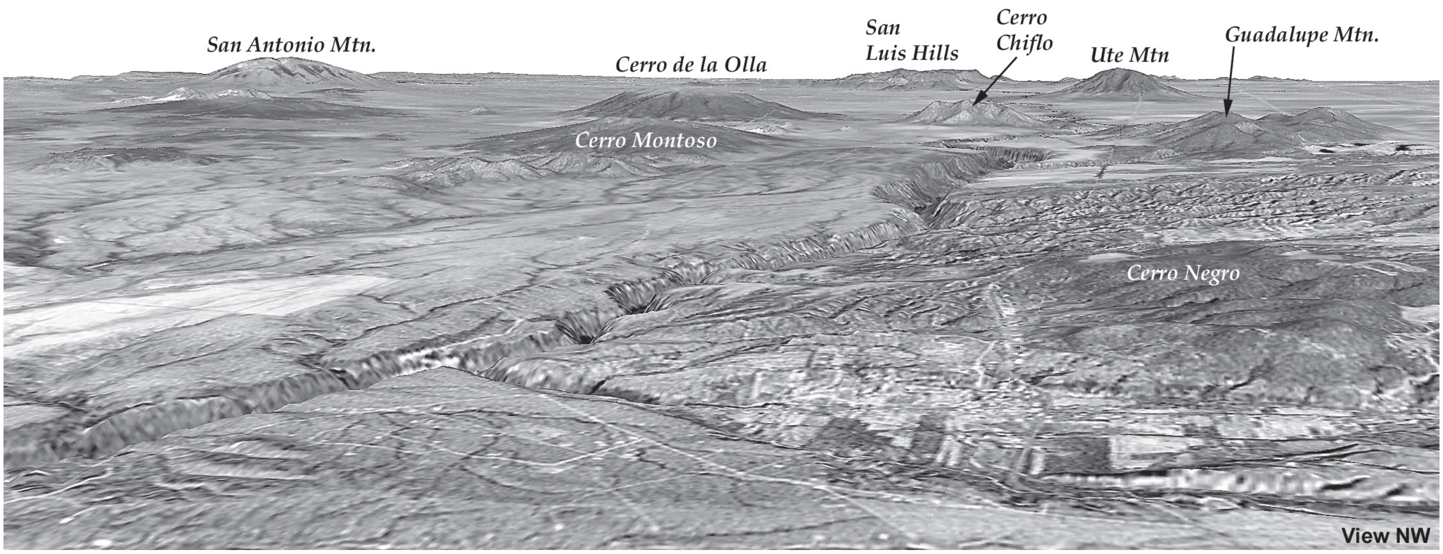

FIGURE 1.3. Virtual view of part of the Taos Plateau volcanic field as might be seen flying north above NM-522. This image constructed from satellite imagery (see Plate 1) draped over a digital elevation model (DEM) and viewed obliquely.

two-pyroxene dacites of the Taos Plateau, these outcrops typically have a dark glassy groundmass (in part due to finely disseminated magnetite) and few plagioclase phenocrysts. **0.1**

18.4 San Cristobal turnoff on right (B-009) leads to the D.H. Lawrence Ranch. Official Scenic Historic Marker reads: *"Lawrence Ranch. University of New Mexico. The Kiowa Ranch, home of novelist D.H. Lawrence and his wife Frieda in 1924-1925, was given to them by Mabel Dodge Lujan. Frieda continued to live at the ranch after his death and later married Angelo Ravagli. In 1934 they built a shrine for Lawrence's ashes. Aldous Huxley was among the many visitors to the ranch."* **3.2**

19.1 Crossing San Cristobal Creek ("St. Christopher"), one of several deeply incised canyons cut into this highly dissected alluvial fan complex. **0.7**

21.8 Cross Garrapata Canyon ("sheep and cattle tick"). To the east is the burn from the 1996 Hondo Fire that consumed 7525 acres. In 1997, fire-enhanced sediment runoff during summer rainstorms in the Garrapata Canyon watershed created exciting new rapids on the Rio Grande two miles west of here (Fig. 1.4). **2.7**

23.4 Village of Lama ("mud or ooze") is to the right. **1.6**

24.2 Communications tower on right. We are crossing into the Red River fault zone, a set of *en echelon*, northwest-striking, east-down normal faults that form prominent scarps from here to Cerro Chiflo (OPTIONAL STOP 3). **0.8**

24.6 NM-515 to the left leads to the Red River Fish Hatchery. The road descends to the Red River along a northwest-trending scarp of the Red River fault zone. We will see the Red River fault zone again at Mile 38.4 as we drive along the east rim of the Rio Grande gorge. Entrenchment of the Red River exposes a complex stratigraphic section of interfingering lower and middle Servilleta Basalt flows and olivine andesite to dacite lava flows erupted from the Red River volcano (McMillan and Dungan, 1986; Dungan et al., 1989). Immediately west of the State Fish Hatchery olivine andesites at river level are overlain by Servilleta Basalt flows, which in turn are overlain by compositionally variable olivine andesite (52-57% SiO_2) presumed to have erupted from vents east of the hatchery. These lower Red River andesite flows are capped by a thick

FIGURE 1.4. Rapid formed on the Rio Grande by a debris flow from Garrapata Canyon after the 1996 Hondo fire in the canyon watershed. Photograph taken just prior to Paul Bauer experiencing the Rio Grande agitation and rinse cycle.

FIGURE 1.5. USGS orthophoto (image taken 5-October-1997) of the Molycorp mill tailings ponds just east of Questa. After the molybdenum is extracted through milling and concentrating at the mine 6 mi east, the tailings slurry is pumped to these tailings ponds via a 9-mi-long steel pipeline along the Red River. The mill tailings contain elevated levels of a variety of metals such as arsenic, cadmium, chromium, cobalt, lead, manganese, and zinc. Elevated levels of sulfate and metals have been found in groundwater in this area and a number of domestic wells have been condemned. Water quality samples collected from tailings pond leachate, ground water, and springs along the Red River indicate that the most likely source for the elevated metal levels are the tailings ponds. Ground water samples collected from up- and down-gradient of the tailings ponds, have indicated that tailings leachate has infiltrated to the shallow aquifer, and that a hydrological connection exists between the ponds and the river. However, to date, surface-water sampling along the river has not found metal concentrations that exceed Federal or State water quality standards.

dacite lava flow erupted from a vent northwest of the hatchery but interpreted to be part of the Red River magmatic system (see Plate 10). **0.4**

25.4 On the distant skyline ahead are the northern Sangre de Cristo Mountains in Colorado. At 11:00 is Guadalupe Mountain, a pair of ca. 5 Ma rhyodacite volcanoes. **0.8**

25.6 Tailings ponds (Fig. 1.5), that contain the desiccated tailings slurry from the Molycorp molybdenum mine, are visible in the foreground ahead. These ponds, and the steel pipes that feed them, have had an ignoble history, beginning with trout-killing slurry leaks in the 1960s. The company has repeatedly been fined by the state for slurry leaks into the Red River, acequias, and farmlands. Ground water beneath the unlined tailings ponds has apparently been contaminated by the downward-percolating slurry. In 1968, Molycorp dedicated the tailings pond (named "Turquoise Lake") at a formal ceremony. In preparation for the ceremony, the company stocked the pond with 2000 pounds of trout and finalized its plans to open the area to the public as a recreational lake. On the morning of the dedication, the 4th of July, hundreds of dead fish were scooped out of the pond, after which the "lake" was permanently closed to the public. When the ponds were allowed to dry in the late 1970s, winds blew clouds of tailings dust into Questa, reportedly causing respiratory problems. When a dust storm covered nearby Questa High School, shutting down a state championship baseball game, students marched on the mine in protest. In 1989, in order to avoid the dust problem, a new high school was built on property purchased at a discount from Molycorp, reportedly at below-market value. Since then, most of the tailings are kept covered with soil for interim reclamation and the sites of active use are rotated (see minipaper by McLemore and Wagner, p. 8). **0.2**

27.0 Crossing over the Red River (named for the color of the water after heavy rains) and entering the Village of Questa, originally named San Antonio del Rio Colorado when officially founded in 1842 and renamed Questa when the post office opened in 1883. The name is probably a corruption of the spanish word *cuesta,* which means slope or grade (Julyan, 1996). **1.4**

27.3 Molycorp 'Sugar Shack West' wasterock pile visible at 1:00, hydrothermal alteration scars visible on the hill ahead. **0.3**

28.2 Junction with NM-38 on right to Red River. Continue north on NM-522. **0.9**

28.5 The right pullout just past the Fire Department pro-
[7] vides a splendid overview of the Taos Range and the Questa caldera and is the site of Optional STOP 5 on the return leg of this log. **0.3**

29.0 The prominent hydrothermal alteration scar visible along the range front of the Sangre de Cristo Mountains at 3:00 occurs in the highly fractured and faulted, 25 Ma, intracaldera Amalia Tuff of the Questa magmatic system (see minipaper by McLemore et al., p. 19). **0.5**

29.4 We are on the most extreme Bouguer gravity low anywhere in the Rio Grande rift (see Plate 3). The low probably represents the down-faulted western portion of the Questa caldera. **0.4**

MOLYCORP TAILINGS FACILITY, QUESTA, NEW MEXICO

Virginia T. McLemore[1] and Anne Wagner[2]

[1]New Mexico Bureau of Geology and Mineral Resources, New Mexico Tech, Socorro, NM 87801, [2]Molycorp, Inc., Questa, New Mexico

The Molycorp tailings facility is located west of Questa, nine miles west of the Questa mine and mill (Figure 1.5). Ore is mined underground then crushed and processed using froth flotation at the mill. The tailings, which are the remaining material after the molybdenum ore is separated, are transported to the tailings facility as a slurry with 38% solids via two 14-inch diameter rubber lined pipelines. The mill process adds lime and other reagents. The tailings that are transported typically range in pH from 7 to 9. The tailings are impounded in two deep arroyos behind earthen-filled dams that cover an area of approximately 640 acres (Wels et al., 2000).

The tailings facility and the nine-mile pipeline were built in 1965 following the development of the open-pit mine. Since 1965, approximately 100 million tons of tailings have been placed in the tailings ponds. The eastern portion of the tailing facility is constructed on recent alluvial sediments, whereas the western portion of the facility is constructed over alluvial sediments and rhyodacite volcanic rocks of Guadalupe Mountain. The permeability of the underlying rocks and unconsolidated alluvial sediments varies from high to low (Wels, et al. 2002).

The tailings facility is currently operated so only relatively small cells (approximately 100 acres) of tailings are exposed at one time. As areas are no longer needed for current operations, interim reclamation occurs. Areas not in current use are covered with soil, an alluvial-gravel material borrowed from the area. Approximately 9 to 12 inches of cover are placed on the tailings and reseeded for interim reclamation. These areas can and will be re-used for future tailings deposition.

About two-thirds of the tailings can be considered coarse tailings, which are defined as less than 50% fines. Fines are silt and clay sized particles smaller than 0.075 mm. Fine tailings (silt size, less than 30% clay) comprise less than 12% of the tailings (Wels et al. 2000). Mineralogically, the tailings consist predominantly of quartz, plagioclase, feldspar, potassium feldspar, and biotite with lesser amounts of chlorite, amphibole, calcite, and sulfide minerals (minor pyrite and molybdenite with trace amounts of chalcopyrite, galena, and pyrrotite). Despite a concentration of 0.5 to 1.5% pyrite in the tailings, no acid rock drainage has been detected (Wels et al., 2002). Paste pH of tailings samples typically ranges from 7.0 to 8.0 and acid buffering minerals such as calcite occur in the tailings. Seepage from below Dam No. 1A in places exceeds New Mexico Water Quality Control Commission (WQCC) ground water standards for sulfate, manganese, molybdenum, Total dissolved solids (TDS) and occasionally fluoride. This water is collected through extraction wells and seepage barriers and discharged under the USEPA National Pollutant Discharge Elimination Permit (NPDES) and is regulated under a New Mexico Environment Department (NMED) ground water discharge permit.

Final closure of the tailings facility under the current permits will include dry closure, with a cover of up to three feet of alluvial material placed over the tailings. The purpose of the cover is to prevent erosion, provide a growth media for vegetation, and provide a store and release cover to reduce water infiltration through the tailings (Robertson Geoconsultants Inc., 2000; Wels et al., 2001). A store and release cover is designed to store water during wetter periods, but allows the release of water by evapotranspiration during drier periods. Store and release covers have been proven effective for semi-arid and arid climates (Wels et al., 2001).

The vegetation in the region is dominated by big sagebrush, chamisa (rubber rabbitbrush) western wheatgrass, and blue grama. Associations in the lower elevations include big sagebrush/western wheatgrass, pinon-juniper and sagebrush. At higher elevations Ponderosa pine begins to occur (Molycorp, 2000).

Lysimeter test plots have been constructed to measure infiltration through cover and tailings, both *in-situ* and reconstructed in the lysimeters. Concurrent monitoring of climatic conditions at the site will allow development of a soil-atmosphere model, which will allow prediction of net infiltration (Wels et al., 2001). At the end of these studies, a comprehensive cover evaluation will allow determination of the cover thickness required for final reclamation and closure at the site.

REFERENCES

Molycorp, Inc., 2000, Wildlife Evaluation for Closeout/Closure of the Molycorp Tailings Facility Questa, New Mexico: Report, 54 p., <http://www.molycorp.com/hes/reports/wild_life_evaluation.html> (accessed on February 16, 2004).

Robertson Geoconsultants Inc., 2000, As-Built Report - Storage Cover Test Plot Study, Questa Tailings Facility, New Mexico: Robertson Geoconsultants Inc., Report No. 052010/5, 27 p., <http://www.molycorp.com/hes/reports/as_built_report.html> (accessed on February 16, 2004).

Wels, C., Shaw, S. and Royle, M., 2000, A Case History of Intrinsic Remediation of Reactive Tailings Seepage for Questa Mine, New Mexico: ICARD 2000 Conference, Proceedings, p. 441-458, (see: <http://www.robertsongeoconsultants.com/papers/ICARDpaper.pdf > (accessed on February 16, 2004).

Wels, C., O'Kane, M., and Fortin, S., 2001, Assessment of Water Storage cover for Questa Tailings Facility, New Mexico: American Society for Surface Mining and Reclamation, Land reclamation: a different approach, Proceedings, v. 2, p. 500-513, (see <http://www.robertsongeoconsultants.com/papers/WScover_ques.pdf > (accessed on February 16, 2004).

Wels, C.; Fortin, S.; Loudon, S., 2002, Assessment of store-and-release cover for Questa tailings facility, New Mexico: Tailings and Mine Waste '02, proceedings of the Ninth International Conference on Tailings and Mine Waste, p. 459-468, (see <http://www.robertsongeoconsultants.com/papers/welaos.pdf> (accessed on February 16, 2004).

30.8 **Turn left** on to NM-378 towards Cerro at "Wild
[8] Rivers" sign. Straight ahead are the twin peaks of Guadalupe Mountain. North and south Guadalupe volcanoes are compositionally similar dacites containing few pyroxene and plagioclase phenocrysts in a characteristically dark glassy groundmass. Lava flows from south Guadalupe Mountain volcano overlie flows from the Red River edifice just north of the Red River gorge. **1.4**

31.6 Ute Mountain 10,093 ft (3076 m) is visible at 11:00 (Fig. 1.6). This Pliocene dacite volcano provides critical riparian and breeding habitat for elk, antelope, peregrine falcon, golden eagle, brown trout, and the federally listed endangered southwestern willow flycatcher and threatened bald eagle. 7924 acres along the western and northwestern flanks of the volcano were recently acquired by the Bureau of Land Management (BLM) through an agreement with private landowners and facilitated by the Trust for Public Lands. Located within the Rio Grande Wild & Scenic River corridor, the BLM will manage the land to protect its open space, recreational, and wildlife habitat values. As of this writing, most of the area is closed to public access while the BLM is formulating a management plan for the land (Bureau of Land Management, 2003). **0.8**

32.1 Church on right is San Antonio de Padua built around 1860. **0.5**

33.8 Mile Marker 3. San Antonio Mountain is ahead on the skyline and at 3:00 the Sangre de Cristo Mountains in Colorado are visible on a clear day. **1.7**

34.2 Cattle guard. Good view of the Taos Plateau volcanoes. The San Luis Hills are in the middle distance at 1:00-2:00, and, on a clear day, the San Juan Mountains are in the far distance. San Antonio Mountain is ahead on the skyline. Cerro de la Olla is ahead in the middle distance. The steeper and more rugged peak at 11:00 is Cerro Chiflo. **0.4**

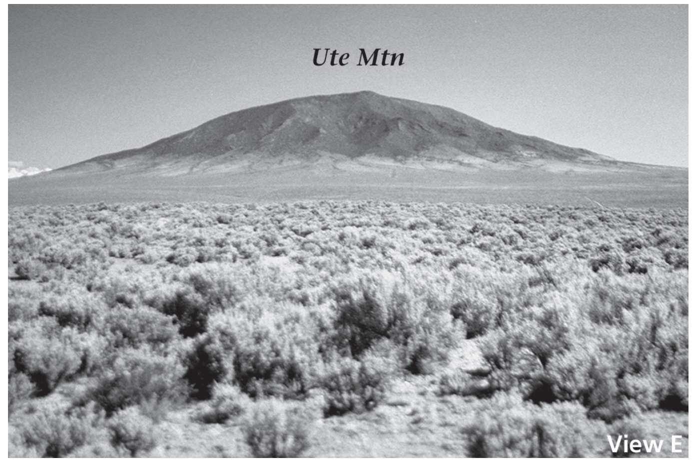

FIGURE 1.6. View of Ute Mountain, a pleasingly symmetric Pliocene dacite volcano just south of the Colorado border.

34.6 Cerro Montoso is now straight ahead. **0.4**

36.2 Entrance to BLM Wild Rivers Recreation Area (cattle guard, fence, and BLM sign). "Sheep Crossing" trail is just ahead. **1.6**

37.0 Chiflo Campground is on the right (site of STOP 4 on
[9] return trip). **0.8**

38.1 Guadalupe Mountain trailhead is on the left. **1.1**

38.4 Tree-covered fault scarp ahead of the Red River fault system, a series of northwest-striking *en echelon* faults that die out to the northwest against Cerro Chiflo. Bear Crossing Campground (just ahead) is the site of OPTIONAL STOP 3 where the fault can be viewed. **0.3**

38.9 Bear Crossing Campground on right, road begins
[10] climb up fault scarp. **0.5**

39.3 Now driving on the top of the footwall block and upper basalt flow. **0.4**

SIDEBAR 1.2 - Wild Rivers Recreation Area was set aside to help you experience the beauty of two national Wild and Scenic Rivers that are protected by Congress. This BLM-administered area is open year round, although winter access may be difficult due to snow-packed roads. Here the Rio Grande and Red River are preserved in their natural, free-flowing state. The Rio Grande has sliced an 800-foot deep canyon through the thick volcanic rocks of the Taos Plateau. The Wild Rivers Backcountry Byway winds its way along the rim of the Rio Grande gorge, providing access to spectacular overlooks including the confluence of the Red River and the Rio Grande below La Junta Point. The area also contains bike trails, trail access to the rivers below, camping, fly fishing, and a variety of hikes. The Visitor Center has bathroom facilities, books, and information. Weekday use is very low and provides great opportunities for solitude, as well as some of the most dramatic views in the state. This area is an excellent alternative to the more crowded Forest Service campgrounds between Questa and Red River.

The canyon ecosystem, from rim to river, creates a unique diversity in plant and animal life. Ancient piñon and juniper forests contain 500-year-old trees. Wildlife includes mule deer, red-tailed hawk, mountain bluebird, and prairie dog. The climate is semi-arid with summer thunderstorms common in July and August, and snow possible from November through March. Summer temperatures range from 45 to 90°F and in winter from –15 to 45°F.

40.4 Wild Rivers pay station on right (site of STOP 2).
[11] The fees collected here are a result of the so-called "Recreational Fee Demonstration Program." Originally authorized in 1996 by a rider on an appropriations bill as a three-year pilot project, the "Fee Demo" program, as it is commonly called, has been reauthorized by Congress through September 2004. The program was intended to alleviate chronic underfunding of public lands management agencies and allows 80% of fees collected to remain on-site. However, the program has drawn wide criticism for what are essentially entrance fees to public lands and for the high costs of overhead for collection and enforcement. Critics also claim that these fees amount to double-taxation and are regressive since they disproportionately affect the poor, especially in rural areas. As of this writing, diametrically opposed bills are before Congress on this issue; one bill would make this program permanent and one would abolish it in all but National Parks. **1.1**

41.6 Some of the 328 million tons of waste rock from the Molycorp molybdenum mine are visible up the canyon to the east (Fig. 1.7). The Mine Rock Pile Stability Review Board, an international team of engineering experts assembled by the State of New Mexico, reported in June 2003 that waste rock piles at the Molycorp Questa mine "pose an immediate public safety issue that needs to be addressed." The report stated that extreme wet conditions could result in "large-volume, high-velocity" slide involving portions of the 360 million tons of waste rock on slopes adjacent to NM-38 and the Red River. According to the report a catastrophic slide could wipe out the mine administration buildings, cross the highway and river, "and up the opposite side of the valley, then downvalley along the highway to the mouth of the canyon and possibly beyond." As this road log was being completed, the state approved Molycorp's four-phase mitigation plan for stabilizing the Goat Hill North rock pile. **1.2**

41.9 **Stay right** at fork in road. The left fork leads to the
[12] BLM Wild Rivers visitor center. The BLM has developed a 5.2-mile Red River Fault trail that begins just west of the visitor center. The trail crosses an impressive northeast-facing fault scarp, and may be the only public trail in New Mexico that is named for a geologic fault. **0.3**

42.3 Passing the Chawa Launa overlook on the right. This overlook provides another spectacular view of the Rio Grande gorge. **0.4**

42.7 Big Arsenic trailhead turnoff on right. The trail descends 680 feet over a distance of 0.7 mi. to the Rio Grande. Big Arsenic Spring is a perennial spring located along the base of the east wall of the gorge. The spring discharges cool water from basin-fill sediments interbedded with Servilleta Basalt flows. Contrary to its name, Big Arsenic Spring discharges high-quality potable water (the false advertising might have been a hermit's attempt to discourage visitors). **0.4**

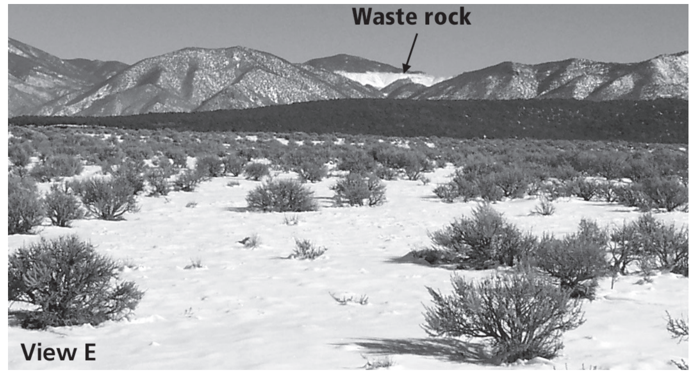

FIGURE 1.7. View eastward of Sangre de Cristo Mountains from the Wild Rivers Recreation Area. Note the white (snow-covered) 'Sugar Shack West' waste-rock pile from the Molycorp molybdenum mine on the Red River. Recent measurements on the 'Goat Hill North' waste-rock pile (not visible here) have shown the ~191x106 m3 pile to be creeping downward. There is concern that a period of intense monsoon rainstorms could potentially trigger a catastrophic collapse of the pile. Molycorp is currently planning remediation to occur in 2004-2005.

43.4 Entrance to Little Arsenic Campground. This trail descends 760 feet over a distance of 1.0 mi. to the river. Little Arsenic Spring is another perennial spring situated approximately 170 ft above the river on the east gorge wall in a sediment zone interbedded with Servilleta Basalt flows. It also discharges cool, high quality water. The large number of springs that discharge along the eastern wall of the Rio Grande gorge probably represent old(?) perched groundwater derived from recharge in the Sangre de Cristo Mountains. **0.7**

43.5 Montoso Campground on the right. **0.1**

44.0 **Turn right** onto dirt road and follow sign to 'La Junta
[13] Point' (an overlook of the 'junction' or confluence of the Red River and the Rio Grande). **0.5**

44.3 STOP 1 - La Junta Point
[14] **Park in lot.**

Walk through picnic area to La Junta Point above the Red River and Rio Grande confluence. La Junta trail descends 800 feet over a distance of 1.2 miles to the confluence, where a footbridge across the Red River provides access downstream of the confluence. **0.3**

This stop provides an introduction to the field conference, an overview of the Taos Plateau, the Taos Plateau volcanic field, and a splendid view of the gorges of the Red River and Rio Grande. Topics of discussion will include the geologic setting of the southern San Luis Basin, the geometry of the Taos graben, the Taos Plateau volcanic field, the geomorphic history of the Rio Grande and Red River, and water quality and quantity issues on both rivers.

What can be seen from here?

La Junta Point provides one of the most spectacular views in the

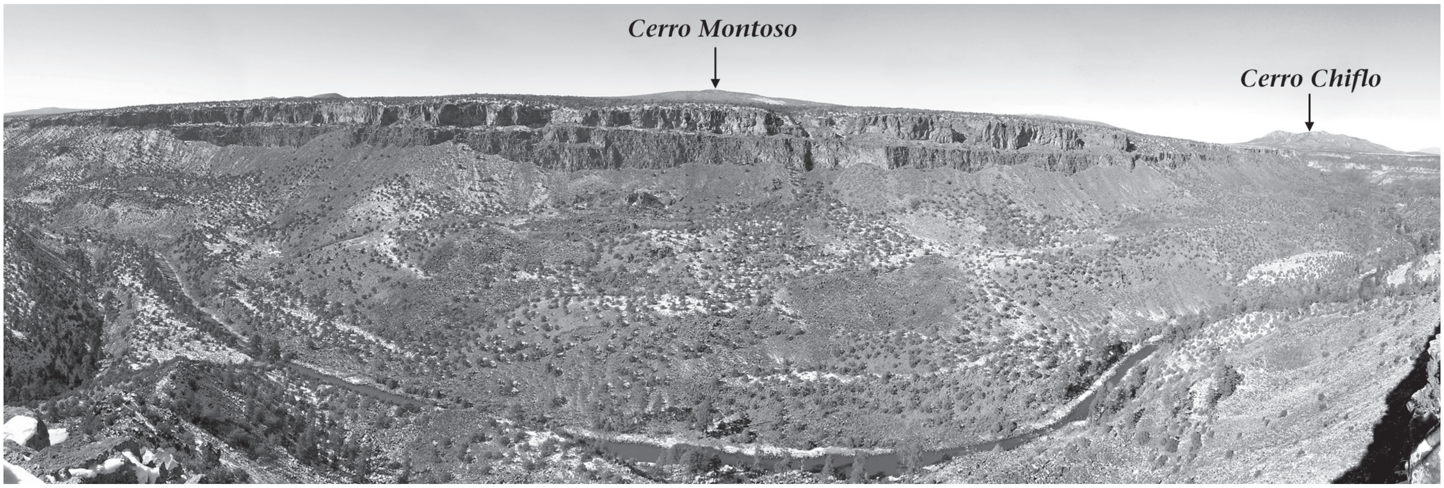

FIGURE 1.8. Panoramic view (~180^o) of the west wall of the Rio Grande gorge from STOP 1. The Red River confluence is at far left, and Cerro Chiflo is on the skyline at far right. The rim of the gorge is formed by a cliff of the UCEM (unnamed cerrito east of Cerro Montoso) dacite lava that overlies flow-packages of both middle and lower Servilleta Basalt. The UCEM flows are overlain by thin flows of the upper Servilleta Basalt that are barely visible. Landslides and talus cover most of the canyon walls here.

state, and it's not even on top of a mountain! To the south, the deeply incised Rio Grande and Red River join in geomorphologically dramatic twin canyons. On the Taos Plateau west of the gorge are the topographically conspicuous Pliocene and smaller Miocene volcanoes of the Taos Plateau volcanic field. In the far distance westward are the Tusas Mountains of the Brazos uplift, the topographic west flank of the east-tilted San Luis Basin. To the east, the topographic and structural edge of the basin is the Sangre de Cristo fault zone that runs along the piedmont of the steep slopes of the Sangre de Cristo Mountains.

Across the gorge to the west (Figs. 1.8 and Plate 10) are cliff exposures of many of the lavas of the Taos Plateau volcanic field. The Servilleta Formation of Butler, (1946), formalized by Montgomery (1953), was redefined by Lipman and Mehnert (1979) as Servilleta Basalt exclusive of the unspecified Santa Fe Group sediments interbedded between flow-packages. We prefer to use the latter terminology to emphasize the volcanic stratigraphy and similarity of these diktytaxitic olivine tholeiites (see Taos Plateau volcanic field discussion below). The UCEM (the "*u*nnamed-*c*errito-*e*ast-of-Cerro-*M*ontoso") dacite lava flows (Dungan et al., 1984) at the top of the gorge overlie flows of the lower Servilleta Basalt (LSB) and middle Servilleta Basalt (MSB), but are overlain by the upper Servilleta Basalt (USB). The three Servilleta Basalt flow-packages represent multiple coalesced flows that form a recognizable stratigraphy throughout the Taos Plateau. Sands and gravels of variable thickness typically separate the three main packages of flows of the Servilleta Basalt and often form slopes between benches of basalt.

The volcanic section at the mouth of the Red River is relatively thin and overlies a thick gravel pile that probably represents the ancestral Red River alluvial fan. Downriver, flows of the LSB and MSB are at a lower elevation, and separated from flows of the USB by a thick section of fluvial gravels. The southern locus of deposition of post-MSB alluvial sedimentation is due to deflection by the Red River shield. The wide belt of landslides at the point is the result of the thick gravels deposited by the Red River. Upstream, the canyon narrows and steepens as the effect of the fan diminishes.

The capping UCEM dacite flow across the canyon to the west is not present on our side. The Rio Grande apparently went around the east end of it. The dacite both downstream and upstream is overlapped by the USB sequence. Note that the surface of the plateau upstream to this point is fairly level, but at the junction it tilts south to the Dunn fault (a height difference of about 500 feet). Below the Dunn fault the plateau surface along the river is relatively level again.

The view up Red River to the andesite sequence is blocked by the nearer curves in the canyon. They are visible from the trail at the El Aguaje Campground. At that viewpoint one of the Red River faults can be seen that has a thicker section of both volcanic and sedimentary rocks on the downthrown side.

This spot represents a special place in the history of the Rio Grande, as prior to the mid-Pleistocene the headwaters of the Rio Grande were actually the Red River, and the watersheds north of here once emptied into a large lake in the Sunshine Valley (Wells et al., 1987). The integration of these northern drainages with the Rio Grande had profound effects on the geomorphic history of all the Rio Grande rift basins (see below).

Geologic setting of southern San Luis Basin:
The Rio Grande rift in northern New Mexico is composed of a series of north-trending, elongate topographic and structural basins, including the San Luis and Española Basins. The basins are broad half grabens that are tilted to either the east or west, and typically have a relatively active, north-striking fault along one border as well as numerous lesser faults within the basin (see Plates 2 and 6). Current tectonic models based on geologic, geophysical, and drill hole data suggest that the basins of the northern Rio Grande rift are separated by northeast-trending zones that accommodate the opposing senses of basin tilting (Chapin and Cather, 1994).

The San Luis Basin (see Plate 3) is one of the major structural elements of the Rio Grande rift. It is approximately 240 km long, and is bordered by the Sangre de Cristo Mountains on the east, and the Tusas and San Juan Mountains on the west. The southern part of the basin is a physiographically and geologically unique terrain known as the Taos Plateau. The plateau is composed mostly of Pliocene basaltic rocks that were erupted locally, and have only been mildly deformed by rift processes. Basalt flows dip very gently to the east, at about 6 m/km or 0.34° (Lipman and Mehnert, 1979). The plateau surface shows only minor dissection, although the Rio Grande and its two major tributaries are confined to deep canyons cut through the volcanic rocks. The 300-m-deep Rio Grande gorge contains good exposures of predominantly Pliocene volcanic rocks, as well as the interlayered sands and gravels of basin fill deposits that represent westward-prograding alluvial fans of the Taos Range (Peterson, 1981; Dungan et al., 1984). Based on surface mapping and drill-hole data, the basalt flows pinch out eastward and southward towards the edge of the basin.

In the Taos area, the Rio Grande rift is a 30-km-wide (20 mi), asymmetrical basin with the major flanking fault system along its eastern border (Sangre de Cristo fault). The total throw on the Sangre de Cristo fault system may be as much as 7 or 8 km (Lipman and Mehnert, 1979). Gravity data indicate that at the latitude of Taos, the basin consists of a deep north-south graben (the Taos graben, perhaps >5 km deep) along the eastern edge of the rift (Cordell, 1978; Bauer and Kelson, 2004, this volume). The structural bench west of the Taos graben rises gently to the Tusas Mountains, and is cut by numerous small-displacement normal faults. To the north, the bench becomes an intra-rift horst with Oligocene volcanic rocks exposed in the middle of the rift at the San Luis Hills of southern Colorado (Lipman and Mehnert, 1979).

The Taos graben:
The Taos graben, which was first recognized by Cordell (1978) from gravity data, is the major structural feature in the Taos area, and probably is the key to deciphering the great variety of surficial geologic and physiographic features in the region. At the latitude of Taos, the north-south graben is approximately 13 km (8 mi) wide. The western edge of the graben (the Gorge fault) lies beneath the Rio Grande (Cordell and Keller, 1984), resulting in a graben that is less than half the width of the topographic valley. The deepest part of the graben is just west of Taos Pueblo, where the depth to Precambrian basement rocks was estimated at over 5000 m (16,400 ft) from gravity data (Keller et al., 1984).

Tectonic surface expression of the Gorge fault zone in the area is scarce. The Dunn Bridge fault, which is exposed in the gorge near the Dunn Bridge, is a normal, east-down, north-striking, 35 m scarp that has formed in the last 3.5 Ma (Dungan et al., 1984). Recent mapping in the Carson quadrangle by Kelson and Bauer (1998) identified an east-facing fault scarp that branches from the Embudo fault near Pilar, and extends northward towards the Dunn Bridge fault. A large number of springs, including Manby hot springs, exist along the Rio Grande between Taos Junction bridge and the Red River confluence. Most likely these springs owe their existence to the buried Gorge fault zone.

The eastern edge of the Taos graben correlates with mapped and inferred structures of the Sangre de Cristo fault zone that will be examined on Day 2. Gravity data as interpreted by Reynolds (1992) showed a complex eastern fault zone that generally steps down into the graben. Reynolds (1986, 1992) also performed shallow seismic reflection surveys over parts of Taos Pueblo, interpreting a complex system of buried faults along the Cañon section of the fault zone, including some small-scale horst and graben geometries. In 1996, the Town of Taos drilled an exploration water well at the Town Yard, southwest of Taos. After drilling through 600 ft of sand and gravel basin fill, a 70-ft-thick basalt was encountered, and at 720 ft Pennsylvanian sedimentary strata were encountered. Drilling ceased after penetrating 300 ft of the Pennsylvanian section. Just to the northeast of the Town Yard well is a spring that is shown on the USGS Taos 7.5-minute quadrangle.

The existence of shallow bedrock and the spring is consistent with a large, NNE-trending structural bedrock high (Town Yard bench) present in the subsurface. The bench corresponds with a strong gravity gradient, and projects northward along the western edge of Buffalo Pasture wetland area of Taos Pueblo (see Day 2, Stop 2). The western boundary fault of the bench also projects southward into the Picuris-Pecos fault system mapped south of the Embudo fault zone (see Bauer and Kelson, 2004a, this volume). There is some inferred surface expression of the western boundary fault (Town Yard fault) of the Town Yard bench. We suspect that this buried structure has an impact on ground water flow in the Taos area, and may represent a reactivated part of the Miranda fault zone to the south. We do not know the exact configuration of the structural bench, but Bauer adn Kelson (2004, this volume) show a speculative interpretation.

Taos Plateau volcanic field:
The Pliocene to Pleistocene Taos Plateau volcanic field (TPVF) in the San Luis Basin of northern New Mexico and southern Colorado is one of the largest and compositionally most diverse volcanic fields of the Rio Grande rift. Rift-related volcanic rocks exposed on the Taos Plateau cover approximately 1500 km^2 and erupted over a five million year period from approximately 6 Ma to 1 Ma (Lipman and Mehnert, 1979; Appelt, 1998). No fewer than 35 discrete vent areas have been identified (see Fig. 1.9 and Plates 1 & 2) during mapping of Rio Grande gorge stratigraphy (Dungan et al., 1984; Appelt, 1998), recent drilling near Taos (Bauer and Kelson, 2004a, this volume), and high-resolution aeromagnetic data east of the Rio Grande (Grauch et al., 2004, this volume) suggest that a number of buried vents may be additional source areas for Taos Plateau lavas. The lava flows and associated pyroclastic rocks span a compositional range from tholeiitic basalts to trachybasalts and basaltic trachyandesites to calc-alkaline andesites, dacites and rhyolites. The geomorphic form of volcanic edifices is broadly correlative with composition; the more evolved dacites typically forming steeper-sided volcanoes and lava domes like Ute Mountain (see Fig. 1.6) and the least evolved tholeiites forming broad low-relief shields (Lipman and Mehnert, 1979). Prominent vent locations for these tholeiites include a cluster of three low

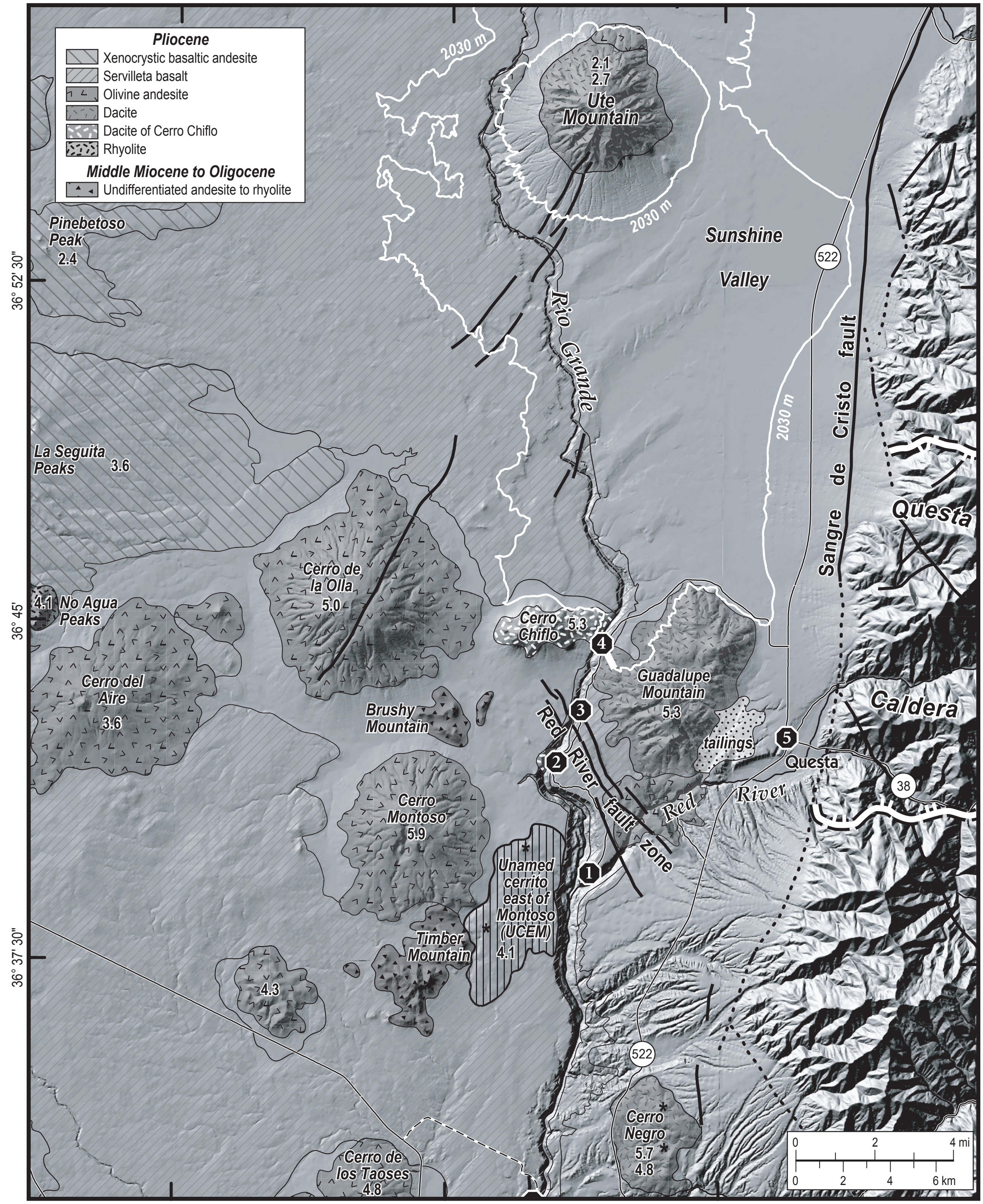

FIGURE 1.9. Geologic map showing volcanic rocks of the Taos Plateau volcanic field draped over 10-m digital-elevation-model image. Average ages (Ma) for Pliocene eruptive centers are shown (McIntosh et al., 2004; Appelt, 1998). In addition to the volcanic features, clearly visible are Rio Grande gorge, Red River Canyon, the Sangre de Cristo Mountain front, and a variety of subtle geomorphic landforms in the area. The 2320 m (7612 ft) contour line is shown to depict a hypothetical maximum lake level for the pre-integration Sunshine Valley Lake. The figure also clearly shows the differences between the highly dissected piedmont south of the Red River, the moderately dissected Taos Plateau west of the Rio Grande, and the relatively undissected piedmont east of the Rio Grande.

shields west of Cerro Montoso, Pinebetoso Peaks, State Line, and unnamed vent areas northwest of San Antonio Mountain. There are a number of exceptions to this observation on the Taos Plateau and they will be noted where appropriate. In light of the geochemical complexity observed in the Taos Plateau lavas (Lipman and Mehnert, 1979; Dungan et al., 1986, McMillan and Dungan, 1988a; McMillan and Dungan, 1988b) the rock classification scheme adopted in the above studies and utilized on this trip is briefly described below.

Olivine tholeiites of the Servilleta Basalt are by far the dominant mafic composition of lavas erupted (>200 km^3) in the Taos Plateau volcanic field. These basalts contain olivine ($Fo_{80.5-83}$)+Cr-spinel±plagioclase phenocrysts in an ophitic-diktytaxitic groundmass (*ophitic*: augite encloses plagioclase; *diktytaxitic*: plagioclase laths bound void space). The development of the diktytaxitic texture allowed the formation of extensive vesicular segregations as pipes and sheets during post-emplacement *in-situ* crystallization. These segregations are enriched in incompatible trace elements and depleted in Ni and Cr relative to massive interiors of the flows (Dungan et al., 1986), and are best developed in flows with the coarsest diktytaxitic groundmass textures.

Olivine andesites of the TPVF (26 km^3) are defined as the calc-alkaline, olivine-bearing intermediate volcanic rocks between 55-60 wt% SiO_2 (McMillan and Dungan, 1988). The andesites occur as weakly to moderately vesicular aa flows and associated near-vent cinder, spatter and agglutinate. The upper SiO_2 content of the olivine andesites is defined mineralogically by the reaction (olivine+melt=orthopyroxene) and volcanologically by the monolithologic character of the shield edifices. Andesites contain olivine±plagioclase ±augite±orthopyroxene in an intergranular groundmass. Olivine phenocrysts are euhedral to skeletal, weakly zoned, and in equilibrium with whole-rock compositions, indicating that olivine was the liquidus phase of these magmas. Andesites have Mg-contents equivalent to or only slightly lower than the Servilleta Basalt, precluding fractional crystallization from the basalts as the major petrogenetic process. Incompatible trace elements are enriched in the andesites relative to the basalts, and are comparable to those observed in many of the dacites. Olivine andesite volcanic centers include Cerro del Aire, Cerro de la Olla, Cerro Montoso, and Cerro de los Taoses.

Xenocrystic basaltic andesites erupted periodically throughout the Pliocene to Pleistocene volcanic history of the Taos Plateau and are universally associated with short-lived small volume eruptive centers. In places these eruptions predated major eruptions of more evolved compositions, as in the case of the clustered centers of Los Cerritos de la Cruz and Red Hill southwest of San Antonio Mountain. However, they often appear to be late stage eruptions such as those from the small vents of La Segita Peaks and a similar center on the northeast flank of San Antonio Mountain. These andesites are compositionally very similar to the olivine andesites, but carry numerous xenocrysts of sodic plagioclase and resorbed quartz.

Two-pyroxene dacites, referred to historically in the literature as rhyodacites, form dark gray to black, non-vesicular lava flows containing augite+orthophyroxene+plagioclase in a typically glassy groundmass. Two-pyroxene dacites range in composition from low-silica (60.5 wt% SiO_2) lava flows capping the Red River gorge sequence to high-silica (67.3 wt% SiO_2) flows at Guadalupe Mountain. Other prominent two-pyroxene dacite volcanoes include San Antonio Mountain, Ute Mountain, Cerro Negro, "Unamed Cerrito East of Montoso" (UCEM), and Tres Orejas.

Cerro Chiflo dacite, previously referred to as quartz latite (Lipman and Mehnert, 1979), contains abundant plagioclase+biotite+hornblende phenocrysts and is unlike any other Pliocene dacites of the TPVF. The flow-banded dacite is light brown to gray, wholly devitrified and contains xenoliths up to 10 cm diameter of Precambrian schist, gneiss, and granite (Lipman and Mehnert, 1979). Mineralogically and chemically similar dacites occur at Timber Mountain and Brushy Mountain as part of the Oligocene to Miocene volcanic section on the Taos Plateau.

The rhyolite lava domes at No Agua Peaks are the most evolved lavas of the TPVF (76.5 wt% SiO_2) and are nearly aphyric, containing less than 1% plagioclase+sanidine+quartz (Lipman and Mehnert, 1979). The margins of the domes consist of hydrated perlitic glass with obsidian inclusions (often called "apache tears"). The interiors of the lava domes are flow laminated and mostly devitrified.

Geomorphic history of the Rio Grande and Red River: The present-day Rio Grande flows across two distinct geomorphic regions in southern Colorado and northern New Mexico; the broad San Luis Valley in southern Colorado and the Taos Plateau in northern New Mexico. The boundary between these regions is a zone of multiple Miocene and Pliocene volcanic vents. Wells et al. (1987) identified several lines of evidence suggesting that the two regions (i.e., the San Luis Valley and the Taos Plateau) have different geomorphic histories related to the mid-Pleistocene capture of the San Luis Valley drainage by the ancestral Rio Grande (see Plate 10 and Fig. 1.9). During the early Pleistocene, the San Luis Valley was a closed (or nearly closed) basin, which received water from Latir, Costilla and Culebra Creeks draining the Sangre de Cristo Mountains and from the Conejos and Alamosa Rivers draining the San Juan Mountains. The southern end of this basin was near Cerro Chiflo, in the cluster of Neogene volcanic cones forming the boundary between the San Luis Valley and the Taos Plateau. The northeast-facing fault scarp along the Red River fault zone may have formed the topographic sill at the southernmost end of the basin, based on the presence of a pebble gravel overlying the Servilleta Basalt to the north of the scarp. This pebble gravel contains clasts probably derived from the San Juan Mountains. There are also lake/playa beds overlying the Servilleta Basalt north of the fault scarp (Wells et al., 1987) and farther north in the San Luis Valley (Rogers et al., 1985). South of the Red River fault scarp, there are no fluvial deposits overlying the uppermost flows of Servilleta Basalt until the Red River confluence, where coarse cobble gravel correlative with ancestral Rio Grande gravels (see Plate 10) flank the Red River gorge. Thus, it appears that prior to integration of the present-day Rio Grande, the Red River drainage basin formed the northern headwaters of the Rio Grande. In addition, Wells et al. (1987) noted the presence of a 180-m-high knickpoint in the long-profile of the Rio Grande upstream of the Red River confluence, and interpret this to be related to the capture of the San Luis Valley drainage by the Rio Grande south of Cerro Chiflo. Plate 10 shows the steep gradient of this section of the Rio Grande.

The position of the Rio Grande and its gorge probably is related to the existence of the Gorge fault zone and the western edge of the Taos graben. Dungan et al. (1984) concluded that the position of the river is "controlled by a combination of overall east-tilting of the plateau, westward prograding alluvial fans, and the local control exerted by the faults, which in turn are surface manifestations of the deep Taos graben." The gentle east tilt of the plateau likely forced the ancestral Rio Grande eastward, while the prograding fans probably constrained the amount of eastward migration. Possibly, the Rio Grande incised into the Gorge fault because of a lower resistance related to fractured basalt within the north-trending fault zone.

Red River water quality:
The US Geological Survey and the New Mexico Environment Department entered into a Joint Powers Agreement in April 2001 to investigate the baseline and pre-mining ground water quality in the Red River drainage basin. The main objective is to infer the pre-mining ground water quality at the Molycorp mine site. The study was begun because New Mexico law states that part of the closeout plan for mining sites must include compliance with ground water quality standards unless it can be shown that prior to mining, ground water quality did not meet these standards. There are reasons to believe that pre-mining ground water quality was poor (this is called *Red* River after all), although no quantitative information exists. If these conditions can be reasonably demonstrated and found acceptable to the appropriate parties, then they may be used in lieu of the existing ground water quality standards. The investigation uses a multi-faceted approach to determining pre-mining ground water quality, including determination of the existing hydrogeologic and geochemical conditions at off-site analog areas, modeling of the hydrogeochemical conditions off site, determining parameters that would have affected on-site controls of hydrogeology and geochemistry before mining, and appropriate scaling and modeling of on-site conditions.
[Modified from USGS Web Page: http://wwwbrr.cr.usgs.gov/projects/GWC_chemtherm/questa.htm]

Water from Colorado – Steve Harris, Rio Grande Restoration:
The river below you is an artifact of an elaborately negotiated legal system. Every water molecule which passes by has a legal owner. Almost 90% of surface water withdrawals are for agriculture throughout the upper basin states. The principal crops are alfalfa, pasture and hay. Each year, approximately 40-55% of the Rio Grande flow that reaches Del Norte, Colorado is depleted in Colorado. Under terms of the 1939 Rio Grande Compact, river flows to preserve ecological functions are largely dictated by the obligation of upstream states to supply water to downstream states. Thus, the river's ecological function is entirely incidental to human uses. The Rio Grande frequently runs dry in four reaches in the latter part of the irrigation season (July-October) of dry years. This is compounded by a floodplain infested with thickets of non-native riparian species like tamarisk and Russian-olive that consume a large amount of water. The greatly simplified ecosystem, coupled with draught and human diversions of water, has caused or threatened extinction (or extirpation) of several aquatic species, including the Rio Grande silvery minnow.

Rio Grande water administrators, not to mention the river itself, are burdened by an over-allocation of claims to divert its flows. Colorado is able to comply with its Rio Grande Compact obligations by daily administration of a schedule of priority uses. Junior (more recent) appropriators are curtailed progressively up the priority list, until permitted uses plus Compact obligations equal the available flow. In dry seasons, the Rio Grande in Colorado may serve only the appropriators having 1880 and earlier priority dates. In contrast, New Mexico has never adjudicated a schedule of water-right priorities to Rio Grande flows. New Mexico meets its Compact delivery obligations largely due to return flows from inefficient irrigation in the Middle Rio Grande valley, where each irrigated acre can divert up to 12 acre-feet per year. Irrigation water unused by crops returns to the river and, if luck holds, to storage in Elephant Butte Reservoir sufficient to satisfy Compact obligations.

In an average year, only about 8% of the waters produced by headwaters sources reach Ft. Quitman, Texas, the dividing line between upper and lower Rio Grande basins. Most years, upper Rio Grande water never reaches the Gulf of Mexico at all.

End of Stop 1.
Return to vehicles and backtrack northwards.

44.6 **Turn left onto paved road.** **[13]** **0.3**

44.7 Latir Peak is visible above treeline at 1:30. The name Latir may have been a French surname, or may be derived from the Spanish verb *latir* which means to howl or bark (Julyan, 1996). The peak is composed of massive Tertiary quartz latite lavas (Lipman and Reed, 1989). **0.1**

46.7 **[12]** Stay left at Stop sign, and continue backtracking. The right road leads to the BLM Wild Rivers visitor center. **2.0**

48.1 [11] STOP 2. Wild Rivers Recreation Area Pay Station. Turn left into the parking lot.

Walk due west about 100 meters to the rim of the Rio Grande gorge. At this stop we discuss the buried volcano displayed along the gorge, the general pre-eruptive topography of the area, and the latest radioisotopic ages for the Taos Plateau volcanic rocks. This overlook provides a spectacular gorge cross-section of a cider cone that is onlapped by flows of the middle Servilleta Basalt and capped by upper Servilleta Basalt. **1.4**

The view west across the Rio Grande at this stop (Fig. 1.10) illustrates the significant impact that paleotopography and prograding fan deposits of the Red River alluvial system have on

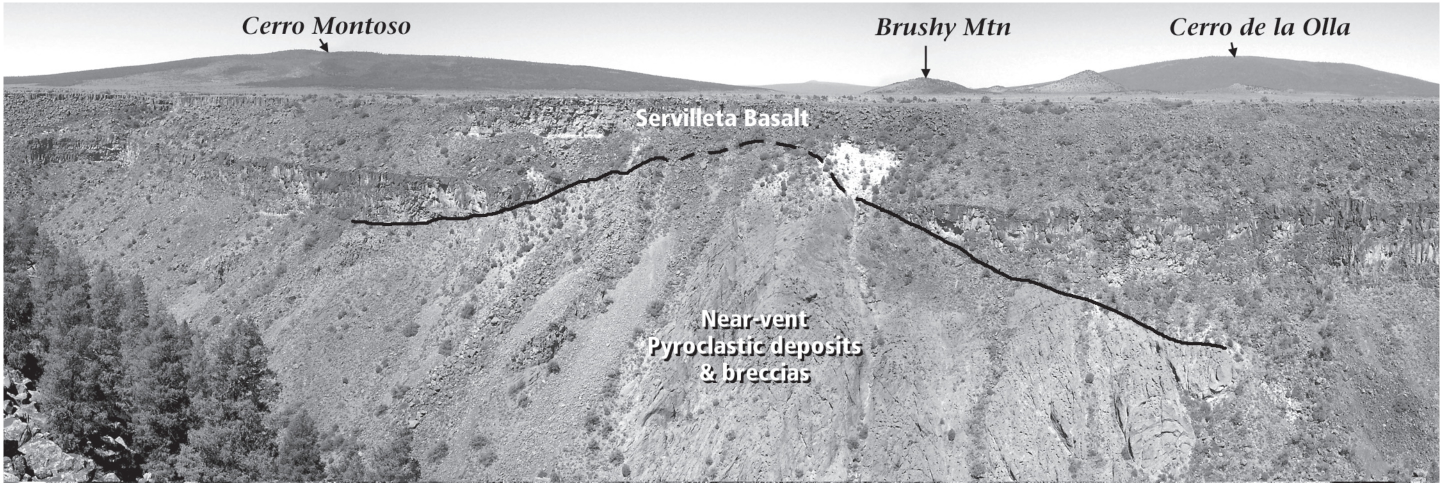

FIGURE 1.10. Panoramic view westward from STOP 2 of the buried volcanic edifice in the Rio Grande gorge wall. This cinder cone, likely related to the Cerro Chiflo eruptions, was onlapped, and ultimately buried by the Servilleta Basalt. The broad Pliocene volcanoes on the skyline are Cerro Montoso on the left and Cerro de la Olla on the right. The small hill between is Brushy Mountain, a structurally high remnant of an early Miocene volcano.

the basin stratigraphy exposed in the gorge. Here, remnants of near-vent pyroclastic deposits and breccias, likely related to the Cerro Chiflo eruptions, formed a paleotopographic high. This had the effect of deflecting prograding fan deposits to the north and south resulting in a thickened sedimentary sequence on either side. Additionally this may have served to restrict flows from the "*u*nnamed-*C*errito-*e*ast-of-Cerro *M*ontoso" (UCEM) and Guadalupe Mountain centers to the south and north of this topographic high, respectively. Note the thickened upper flows (USB) of the Servilleta Basalt that cap the sedimentary section here relative to the previous stop.

Early Rift Volcanism:

Volcanism associated with rifting in the San Luis Valley segment of the Rio Grande rift is believed to have commenced at approximately 26 Ma, nearly coincident with eruption of the 25.1 Ma Amalia Tuff from the Questa caldera. The most compelling arguments for the coincidence of volcanism and extensional tectonism are based on the presence of intercalated basin-fill sedimentary deposits and predominantly mafic lava flows preserved on the western margin of the San Luis Valley in the southeastern San Juan Mountains in Colorado and the Tusas Mountains in New Mexico (Lipman and Mehnert, 1975; Thompson and Lipman, 1994a; Thompson and Lipman, 1994b). Near the Colorado border, on the eastern margin of the rift, remnants of Amalia Tuff overlie Santa Fe Group sedimentary deposits in an early-rift basin stranded near the Sangre de Cristo range-crest; the result of displacement along the Sangre de Cristo fault block (Miggins et al., 2002). Within the San Luis Valley, remnants of older post-26 Ma volcanic rocks are well exposed at three localities along an intrarift structural horst west of the Taos graben: the San Luis Hills in Colorado (Thompson and Machette, 1989; Thompson et al., 1991) and at Brushy Mountain and Timber Mountain in New Mexico (Lipman and Mehnert, 1979; Thompson et al., 1986; Thompson and Schilling, 1988).

The San Luis Hills are a series of flat-topped mesas and irregular hills that trend north to northeasterly for approximately 45 km from the Colorado-New Mexico border (see Plate 2). The stratigraphic sequence exposed here consists of two volcanic assemblages separated by a major erosional unconformity. A thick sequence of 26 Ma basaltic lava flows of the Hinsdale Formation overlie a deeply eroded sequence of andesite and dacite lava flows apparently intruded by cogenetic plutons of quartz monzonite, diorite stocks and hypabyssal dike swarm intrusions. Originally thought to be correlative with the intermediate composition Oligocene lavas and breccias of the 33-29 Ma Conejos Formation (Lipman et al., 1970) in the southern San Juan Mountains, a more recent $^{40}Ar/^{39}Ar$ age determination on biotite from a late-stage dacite dike yielded an age of 27.7 Ma (unpublished age determination by D. Lux and M.A. Dungan, written communication, 1989). This suggests that the older volcanic rocks of the San Luis Hills postdate the inception of major caldera-forming volcanism of the San Juan volcanic field (29-28.2 Ma; Lipman et al., 1996) and is temporally related to precaldera, intermediate-composition volcanic rocks of the Latir volcanic field (Lipman et al., 1986).

Late Oligocene and early Miocene volcanic rocks of Timber Mountain and Brushy Mountain (10 km to the north) on the Taos Plateau constitute a small volume (15 km^2) of post-caldera volcanism of the Latir volcanic field (Thompson et al., 1986). These erosional remnants record two periods of volcanism dominated by eruption of dacitic lavas, but including flows of andesite, rhyolite lavas and ash flow tuffs. Both episodes of volcanic activity appear to post-date 25.1 Ma Amalia Tuff eruption (Smith et al., 2002) and may, based on limited dating, be separated in time by as much as 3 million years. The older sequence is exposed only at Timber Mountain and consists of a 25 Ma basal low-silica rhyolite ash-flow tuff (Lipman and Mehnert, 1975), locally overlain by a cogenetic cone of dacite spatter. Additional remnants of a low-silica rhyolite lava flow and two olivine andesite lava flows are preserved locally. The younger sequence at Timber Mountain is represented by multiple dacite lava flows distinguished primarily on the basis of hornblende proportions relative to plagioclase, pyroxene and Fe-Ti oxide phenocrysts. At Brushy Mountain, outliers of Amalia Tuff are overlain by a 22-Ma high-silica rhyolite dome (Lipman and Mehnert, 1975) which is in turn overlain by an olivine andesite lava flow, a discontinuous flow of aphyric dacite and several hornblende-bearing dacite flows and associated breccias. These stratigraphic relations suggest that the lower volcanic sequences at Brushy Mountain were either stripped prior to eruption of the upper sequence or were never present due to the local nature of the small volume eruptions represented by the older rocks. The deposits attest to the once nearly continuous and predominantly intermediate to silicic volcanic cover that comprised the pre- and early-rift volcanic highland now occupied by the largely Pliocene basaltic volcanism of the San Luis Valley and Taos Plateau.

End of Stop 2.
Return to vehicles, exit lot left, and continue backtracking.

49.2 Descending fault scarp of the Red River fault zone after "Hill" sign. **1.1**

49.7 [10] OPTIONAL STOP 3. Bear Crossing Campground. Turn left into campground.
Walk west to the gorge rim. At this stop we will discuss the geometry and kinematic history of the Red River fault zone. We are just north of the Red River fault zone (Fig. 1.11). North-down scarps are visible on both sides of the gorge to the south of here. The fault zone consists of several *en echelon* fault splays that offset the youngest flows of the Servilleta Basalt and overlying Quaternary gravel. **0.5**

The fault scarp is exposed on the west side of the gorge and is less vegetated than the east side. This northwest-striking series of normal fault strands are about 6 to 13 km west of the rift-margin Sangre de Cristo fault in the southern San Luis Basin. The fault strands have east-down displacement of the Servilleta Basalt, and probably comprise an antithetic structure to the Sangre de Cristo fault. The fault has prominent geomorphic expression where it displaces basalt at the surface, although to the south of the Red River gorge the expression of the fault diminishes, perhaps because of burial by late Pleistocene alluvial-fan deposits (Menges, 1988; Machette et al., 1998). Northeast-facing scarps along the Red River fault zone, and nearby volcanic edifices (see Fig. 1.9), may have formed a topographic sill at the southern end of the San Luis Basin, which, when breached in the middle Pleistocene led to the integration of the Rio Grande below Cerro Chiflo with the San Luis Basin (Wells et al., 1987).

The total vertical separation of the flows of the upper Servilleta Basalt across the Red River fault zone is 30 to 40 m, although different strands within the fault zone show different amounts of displacement of flows within the Servilleta Basalt. Evidence for growth faulting, penecontemporaneous with eruption of the Servietta Basalt includes decreasing offset of flows up-section and abrupt thickness changes of flows and intra-flow sediments across fault strands (Menges, 1988). Quaternary surficial deposits generally are not present across strands of the fault zone, although Menges (1988) and Heffern (1990) show an antithetic, west-facing scarp developed on Quaternary alluvium on the southeastern side of the Rio Grande. Based on the amount of displacement of the basalt and an age of 2.8 Ma (Peterson, 1981), the slip rate on the Red River fault zone is less than 0.2 mm/yr (Machette et al., 1998).

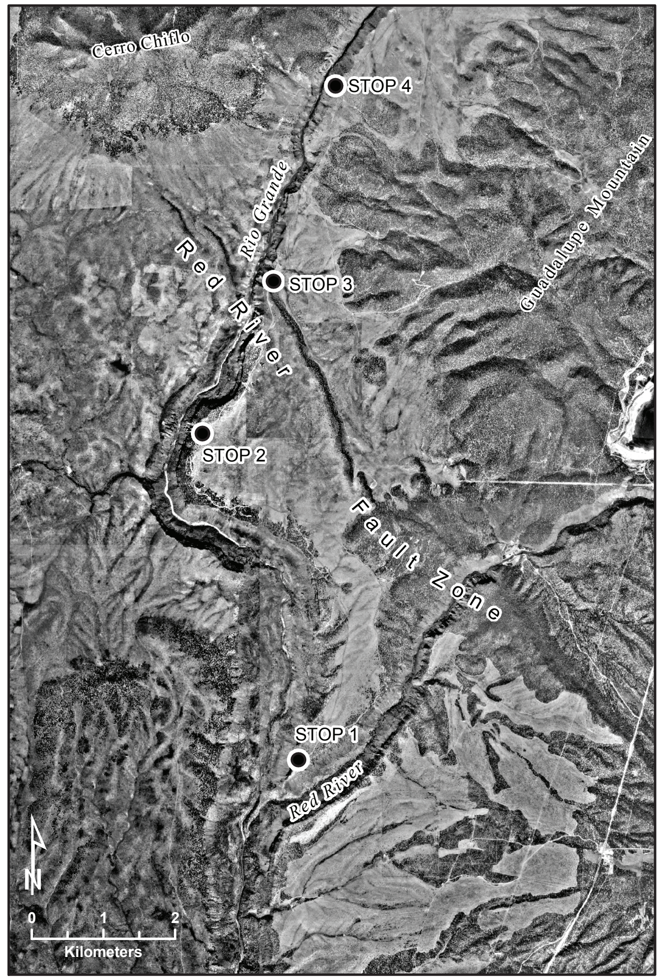

FIGURE 1.11. Digital orthophoto image of the Wild Rivers Recreation Area, taken in 1997, showing the field conference stops in this area and the Red River fault zone. The fault zone consists of a series of northwest-striking, northeast-down, en echelon, normal faults that disrupt the Servilleta Basalt, and possibly some Quaternary deposits. Part of a Molycorp tailings pond is seen along east edge of image.

End of Optional Stop 3
Return to vehicles, exit lot left, and continue northward.

FIGURE 1.12. Panoramic view of the west wall of the Rio Grande gorge at STOP 4. The 5.3 Ma Cerro Chiflo quartz-latite dome has been beautifully exposed by the Rio Grande, including interior, arcuate flow foliations. Flows of the upper Servilleta Basalt onlapped the volcanic edifice and are clearly visible along both sides of the exposed dome.

51.5 STOP 4. Chiflo Campground.

[9] Turn left into the parking lot.

Walk 100 m north (upstream) to view part of the Chiflo volcano in cross section and to discuss inter-related river incision, faulting, and volcanism. The Chiflo trail to the Rio Grande descends 329 vertical feet over a distance of 0.4 miles. The 5.3 Ma Cerro Chiflo quartz latite dome forms a significant nickpoint on the Rio Grande. Upstream, the river gradient is low. Downstream, the gradient is high, and river has cut the deepest section of the gorge. The gorge exposure of the dome clearly shows that flows of the Servilleta Basalt as well as Guadalupe Mountain rhyodacite have lapped against the dome (Fig. 1.12). **1.8**

Chiflo volcano:

Incision by the Rio Grande at this stop reveals a spectacular cross section through the massive interior of the Cerro Chiflo dacite lava dome. Stripped away are any remnants of what likely constituted an extensive brecciated carapace and associated pyroclastic deposits. The lava dome forms a knickpoint in the Rio Grande at this locale resulting in significantly decreased gradient northward. Previously believed to be Miocene in age (10.4 Ma; Lipman and Mehnert, 1979), recent $^{40}Ar/^{39}Ar$ ages reported by Appelt (1998) of 5.32±0.08 Ma suggest nearly contemporaneous eruption with the strikingly dissimilar dacites erupted from the Guadalupe Mountain vents to the east. Cerro Chiflo is a calc-alkaline dacite containing biotite and hornblende in addition to abundant plagioclase phenocrysts. The lava dome is flanked on both sides by flows of Servilleta Basalt presumed to have flowed from vents to the west. Immediately south of Cerro Chiflo, these plateau-forming basalts are capped by the distal lobes of a dacite lava flow believed to represent a late stage eruption from one of the Guadalupe Mountain volcanoes (Dungan et al., 1984).

Story of river capture and integration:

As described at STOP 1, there is geologic and geomorphic evidence (see Figs. 1.9 and Plate 10) that the Rio Grande captured the San Luis Valley drainage area in the mid-Pleistocene (Wells et al., 1987). Based on age estimates from fossils in fine-grained deposits in the San Luis Valley (Rogers et al., 1985) and soils developed on post-Qt2rg terraces near Taos (Kelson, 1986; Kelson and Wells, 1987), this capture probably occurred between about 0.6 and 0.3 Ma. The integration of the large drainage area above Cerro Chiflo (more than about 22,000 km^2) provided a substantial increase in discharge available for erosion and sediment transport, and resulted in rapid incision along the lower Rio Grande into basalts on the Taos Plateau. Incision along fractures zones related to north-striking faults on the Taos Plateau, such as the Dunn fault, resulted in the development of the Rio Grande gorge.

The cause of the capture and integration is unclear, although Wells et al. (1987) speculate that it may have been related to: (1) an overflow of the restricted basin north of Cerro Chiflo and erosion of a channel through *en echelon* scarps of the Red River fault zone (see Fig. 1.11), and/or (2) enhanced incision along the Rio Grande as a result of regional uplift. In both of these cases, the initial incision likely promoted sapping of ground water from the San Luis Valley, which increased contributions to surface water discharge, further promoting downward and headward erosion. As incision progressed northward from Cerro Chiflo, drainages flowing into the San Luis Valley were progressively integrated into the Rio Grande system. This progressive increase in the drainage area of the "new" Rio Grande probably promoted greater incision rates into the Servilleta Basalt, particularly as incision progressed into fracture zones within the basalt.

End of Stop 4

Return to vehicles, exit lot left, and continue backtracking.

52.4 Cattle guard at Sheep's Crossing **0.9**

52.6 Latir Peak (12,708 ft/3,873 m), above treeline at 12:00, is composed of massive Tertiary quartz latite flows and

ALTERATION SCARS IN THE RED RIVER VALLEY, TAOS COUNTY, NEW MEXICO

Virginia T. McLemore[1], Virgil W. Lueth[1], and Bruce M. Walker[2]
[1]New Mexico Bureau of Geology and Mineral Resources, New Mexico Tech. Socorro, New Mexico 87801,
[2]Molycorp, Inc., Questa, New Mexico 87556

More than twenty naturally occurring 'alteration scars' are found along the margins of the Red River between the towns of Questa and Red River. Public and scientific interest in these scars has increased during the last decade because of sporadic but destructive mudslides or debris flows that emanate from the scar areas during wet periods (Meyer and Leonardson, 1990). In addition, water quality degradation of the Red River due to acid, sulfur, and other elements from surface and ground water interaction with these alteration scars has been documented by recent environmental studies (Shaw et al., 2003; Briggs et al., 2003). It is important to study these scars to understand long-term weathering processes and to determine geochemical background of the area.

Alteration scars are natural, colorful (red to yellow to orange to brown), unstable landforms that are characterized by steep slopes (greater than 25^{o}), moderate to high pyrite content (typically greater than one percent), little or no vegetation, and extensively fractured bedrock. The scars are variable in size ranging from one to more than one hundred acres. The distribution of the alteration scars appears to closely follow molybdenum mineralization patterns in the area. However, the relative amounts of hypogene or supergene alteration that may contribute to scar formation is yet undetermined. Many scars are located on south-facing slopes, which tend to have lower vegetation density and snow cover in winter. Erosion of the alteration scars and rapid transport of surface detritus from these areas forms large apron-like debris fan deposits at the base of the scars. Perched ferricrete breccias are found along the margins of some scars.

Most alteration scars are composed of andesite, although other rock types are also found in some scars. The Amalia Tuff (rhyolite) forms the upper portions of some scars, especially those found high on the valley margins. The more competent rhyolite forms near vertical spires, or hoodoos at ridgelines, that are underlain by the weaker andesite and together form a badlands topography due to erosion, rockfall, slumping, landslides, and local down-slope creep of unstable ground.

Preliminary analyses of Airborne Visible-Infrared Imaging Spectrometer (AVIRIS) data indicate that the scars are characterized by abundant jarosite, kaolinite, and locally gypsum, surrounded by a halo of goethite (Livo and Clark, 2002). These secondary minerals are found in addition to common mineral phases, typical of the hypogene quartz-sericite-pyrite (QSP) altered andesite and rhyolite. Within a scar, a progression of grain size reduction is apparent. Within the scars, the rocks are fairly unaltered but highly fractured along the bottom of drainages. Progressing upward, similar in character to soil horizons, the relative sizes of clasts within the profile become smaller and the abundance of clay-size material increases. Secondary minerals (mainly sulfates) typically cement this material during dry periods resulting in a hard surface. With prolonged wetting, this finer material becomes soft and fails readily, sometimes catastrophically.

The high erosion rates on the bare slopes of the scars lead to denudation that continuously exposes additional pyrite-bearing outcrops. Pyrite, when exposed to water, oxidizes and forms sulfuric acid (acid drainage or AD), which then dissolves other minerals in the rock, forming clay minerals as well as soluble sulfate, oxide, and hydroxide minerals. The dissolved constituents form additional acid drainage that mixes with surface and ground water that ultimately enters the Red River. Soils in the alteration scars have average paste pH of 2.5, paste conductivities greater than 1000 μS/cm and sulfate concentrations ranging from 1 to 11.5 percent (Shaw et al., 2003; Robertson GeoConsultants, Inc., 2000a, 2000b, 2001). Leach extractions of samples from the alteration scars show elevated concentrations of S, Cu, F, Bi, Sn, Mn, K, and Th (Robertson GeoConsultants, Inc., 2000a, 2000b; Shaw et al., 2003).

The debris fan deposits shed from the alteration scars consist of varying mixtures of interbedded fluvial, alluvial, and mudflow deposits. The buildup of these deposits in the bedload of the Red River impedes river flow and results in lower stream gradients upstream of the constrictions where meadows are present along the river (Meyer and Leonardson, 1990). The town of Red River, the Questa mill, and Fawn Lakes are built upon such meadowlands.

REFERENCES

Briggs, P. H., Sutley, S. J., and Livo, K. E., 2003, Questa baseline and pre-mining Ground Water Investigation: 11. Geochemistry of Composited Material from Alteration Scars and Mine-Waste Piles: U. S. Geological Survey, Open-file Report 03-458, 17 p.,<http://publs.usgs.gov/of/2003/ofr-03-458/>.

Livo, K. E. and Clark, R. N., 2002, Mapped Minerals at Questa, New Mexico, using airborne visible-infrared imaging spectrometer (AVIRIS) data - preliminary report: U. S. Geological Survey, Open-file Report 02-0026, 13 p., <http://pubs.usgs.gov/of/2002/ofr-02-0026>.

Meyer, J. and Leonardson, R., 1990, Tectonic, hydrothermal, and geomorphic controls on alteration scar formation near Questa, New Mexico: New Mexico Geological Society, Guidebook 41, p. 417-422.

Robertson GeoConsultants Inc, 2001. An Integrated Geochemical Load Balance for Straight Creek, Sangre de Cristo Mountains, New Mexico. RGC Report 052008/13, January, <http://www.molycorp.com/hes/reports/integrated_geochemical.html>.

Robertson GeoConsultants Inc, 2000a. Interim Background Characterization Study, Questa Mine, New Mexico. RGC Report 052008/6, <http://www.molycorp.com/hes/reports/interim_back_characterization.html>.

Robertson GeoConsultants, Inc., 2000b, Background study data report, Questa Mine, New Mexico: Robertson GeoConsultants, Inc. Report 052008/12, January, <http://www.molycorp.com/hes/reports/interim_back_characterization.html>.

Shaw, S., Wels, C., Robertson, A., Fortin, S., and Walker, B., 2003, Background characterisation study of naturally occurring acid rock drainage in the Sangre de Cristo Mountains, Taos County, New Mexico; in 6th ICARD: Cairns, Queensland, Australia, July 12-18, p. 605-616, (see <http.//www.roberstongeoconsultants.com/papers/icard03back.pdf>.

domes. The peak is located within the spectacular 20,506 acre Latir Peak Wilderness of the Carson National Forest, with three peaks over 12,500 feet that display alpine-tundra ecology. Most of the area is drained by the Lake Fork of Cabresto Creek which originates at Heart Lake and is impounded just outside the wilderness in Cabresto Lake, the main trailhead for those going into the wilderness. Many species of wildlife indigenous to the Hudsonian zone of the Southern Rocky Mountains can be found in this remote and spectacular area. The scenic Latir Lakes are located to the north of this wilderness on private land. **0.2**

54.3 Cattle guard. **1.7**

57.2 Ahead on the mountainside is the burn scar of the Hondo fire that was started on May 5, 1996 by a man burning trash in San Cristobal. Whipped by high winds, the fire raged across nearly 8000 acres in 10 hours, incinerating 27 buildings in the community of Lama, displacing 2000 nearby residents, and causing a three-day evacuation of Red River. **2.9**

57.4 Scar in mountainside at 1:00 of yellow hydrothermally altered rocks northwest of MolyCorp Mine (Fig. 1.13) See minipaper by McLemore et al. **0.2**

FIGURE 1.13. View east of the Sangre de Cristo Mountains of a colorful unvegetated outcrop of hydrothermally altered rocks within the 25.1 Ma Amalia Tuff. Such naturally occurring alteration scars are common along the steep slopes of the Red River valley.

57.8 **Turn right onto NM-522** heading south back towards
[8] Taos. **0.4**

60.1 OPTIONAL STOP 5. Fire Station.
[7] **Pull off highway onto the pullout to the right.**

The pullout on the right just past the Fire Department provides a splendid view of the Taos Range and the truncated south margin of the Questa caldera including the structural caldera wall of Proterozoic basement, thick moat-filling welded tuff, and the caldera floor uplifted in a resurgent dome. The geology of the Taos Range is complicated by the juxtaposition of two very different ages of rocks. The Proterozoic basement consists of the highest-grade metamorphic rocks in New Mexico (~ 6-8 kb, 700°C) that, like adjacent ranges, record a polyphase tectonometamorphic history (see minipaper by Dawson, p. 22). These rocks were intruded, and mineralized, by Tertiary volcanic rocks of the Questa Caldera. **2.3**

Latir Volcanic Field and Questa Caldera:

The Latir volcanic field and associated Questa caldera (see Fig. 1.14 and Plate 2) mark the southeastern margin of a formerly spatially contiguous middle Tertiary volcanic field that extends northwest to include the San Juan and Thirty-Nine Mile volcanic fields in southern Colorado (Steven, 1975; Lipman, 1988). Volcanism of the Latir volcanic field largely predates extensional tectonism of the Rio Grande rift. Uplift of the Taos Range along the basin-bounding Sangre de Cristo Fault has exposed a remarkable cross section through the Questa magmatic system (Lipman et al., 1986; Lipman, 1988; Johnson et al., 1989; Lipman and Reed, 1989). Truncation of the western margin of the caldera during rifting has buried much of the volcanic record of the Latir volcanic field in the Taos graben along with basin-fill sediments derived from the surrounding Precambrian and Pennsylvanian rocks of the Taos Range. Differential post-Miocene uplift and erosion of the Taos Range has exposed deeper levels of the Questa magmatic system to the south where co-genetic plutons form the range crest. Near the Colorado border, outflow from the Questa caldera, the 25.1 Ma Amalia Tuff (Smith et al., 2002), dips northward beneath basin-fill sediments of the San Luis Valley. The basal Tertiary surface near the Colorado border is represented by volcanic rocks of the Latir volcanic field, which rest unconformably on Precambrian basement. South to Questa this surface projects skyward to elevations nearing 24,300 ft (7400 m; see Fig. 3 of Lipman, 1988).

Precaldera volcanoes of the Latir field were compositionally diverse, ranging from basaltic andesite to rhyolite forming discrete volcanoes now largely obscured by the Questa caldera. Lava flow sequences of andesite to dacite dominated with subordinate occurrences of smaller volume rhyolite lava domes and associated tuffs (Johnson and Lipman, 1988). Ages of precaldera volcanic rocks range from approximately 28 Ma to 26.5 Ma (Lipman, 1988). Collapse of the Questa caldera was accompanied by outflow of the Amalia Tuff and intracaldera accumulation of densely welded ignimbrites within the caldera. The Amalia Tuff is the only regional ash-flow tuff erupted in the Latir volcanic field and distal remnants are preserved as far north as the Colorado border near the crest of the Sangre de Cristo Mountains (Miggins et al., 2002) and 40 km southwest near the town of Tres Piedras on the western margin of the Taos Plateau. Additional outcrops are preserved at Brushy Mountain along the intrarift horst 14 km east on the Taos Plateau. The Amalia Tuff is a regionally distinctive peralkaline rhyolite containing 10-15% phenocrysts of quartz and sodic sanidine. Recently published ages for the Amalia Tuff are 25.1 Ma (Smith et al., 2002) and 25.0 Ma (Miggins et al., 2002).

From south to north, the high mountain at 1:30 is Flag Mountain (11945 ft / 3640 m), underlain by Proterozoic quartz monzonite. The north shoulder of the mountain, at 1:00 is part of an east-trending alignment of Tertiary granitic to aplitic ring intrusions along the southern margin of the Questa caldera. The switchback roads on the west flank of the mountain provided access to drill pads that were used by Molycorp to block out a large, low-grade molybdenum deposit. The caldera is dissected by two major east-west drainages, the Red River to the south (mile 27.0) and Cabresto Creek to the north. The high ridge between the two drainages consists entirely of densely welded intracaldera Amalia Tuff, rotated to nearly vertical, with an approximate aggregate thickness of 2 km. North of Cabresto Creek is Pinabete Peak (11,946 ft / 3641 m) consisting of volcanic remnants of the caldera floor uplifted during post-caldera resurgence. Precambrian rocks underlying the floor of the caldera form the lower slopes of Pinabete Peak. The prominent hill up Red River Canyon is Goat Hill, which is composed mainly of intracaldera welded tuff and interlayered megabreccia slump-blocks of precaldera lava flows. Beneath Goat Hill is the site of the current Molycorp underground mine (see Leonardson et al., 1983). In the far distance, to the right of Goat Hill, above treeline, is the flank of Gold Hill (11,622 ft / 3542 m), composed of a complex succession of Proterozoic mafic/felsic layered gneiss.

In 1895, gold was discovered in Gold Hill, and by 1897, 200 people lived in nearby Amizette where 600 tons/day of gold, silver, copper, and lead were mined (Sherman and Sherman, 1975). Declining ore-grade at Amizette and difficulty getting the ore to mills at nearby Twining, the namesake of the mining district and another boomtown at what is now the site of Taos Ski Valley, lead to the abandonment of the camps by 1903.(Julyan, 1996).

End of Optional Stop 5.
Pull back onto NM-522

60.4 NM-38 intersection. Ahead is a good profile of the high, west-sloping piedmont surface to the south of the Red River drainage. **0.3**

61.6 Crossing the Red River. **1.2**

64.0 Red River Fish Hatchery road (NM-515) on right. **2.4**

65.2 The Lama Foundation on left is a non-denominational spiritual community founded in 1968. The 1996 Hondo fire destroyed about a dozen buildings here. However, the foundation's central meditation center emerged undamaged. Cebolla Mesa Rd. on the right leads to a well-maintained trail down to the Rio Grande, just below the Red River confluence. **1.2**

65.8 At the crest of Garrapata Ridge. Tres Orejas ahead on skyline is the southernmost dacite volcano on the Taos Plateau. The Tres Orejas dacite eruptions are coeval with the youngest dacite eruptions at Cerro Negro and the andesite eruptions of Cerro de los Taoses. **0.6**

66.9 Crossing Garrapata Canyon. **1.1**

69.1 Village of San Cristobal on the left. **2.2**

69.6 Crossing San Cristobal Creek. **0.5**

70.2 Road to D.H. Lawrence Ranch on left. **0.6**

70.7 View of the southern part of the Taos Plateau volcanic field and the Jemez Mountains in the far distance at 1:00. **0.5**

72.7 The view to the south shows the Qf1 fan surface, with the Picuris Mountains on the distant skyline. The Qf1 fan surface slopes gently to the west, reflecting aggradation from the ancestral Rio Hondo prior to development of the Rio Grande gorge. The Rio Hondo valley contains a flight of six well-preserved terraces that record the response of the Rio Hondo to incision of its master stream, the Rio Grande, into the Servilleta Basalt over the past million years or so. **2.0**

73.4 Crossing the Rio Hondo at the village of Arroyo Hondo. Roads on either side of the bridge lead through the village to the confluence of the Rio Hondo and Rio Grande, but are best avoided with a large group. **0.7**

75.0 **Turn Right onto B-007 gravel road at the top of the**
[15] **grade (*this turn is hard to see when heading south, be careful of traffic behind you*).** The gravel road climbs onto Qf1 surface south of the Rio Hondo drainage. **1.6**

75.2 Cerro de los Taoses forms the low-relief, vegetated shield at 12:00. It has a northern and southern vent area and is one of four major olivine monolithologic andesite volcanoes on the Taos Plateau. $^{40}Ar/^{39}Ar$ ages reported by Appelt (1998) support near-contemporaneous eruptions of both volcanoes at approximately 4.8 Ma.

We are driving on the Qf1 fan surface, which slopes gently westward toward the modern Rio Grande gorge (Fig. 1.15). The Qf1 fan surface is graded to an alluvial terrace formed by the ancestral Rio Grande, mapped as Qt1rg by Kelson (1986) and

PROTEROZOIC TECTONIC HISTORY OF THE TAOS RANGE

Jane P. Dawson
Department of Geological and Atmospheric Sciences, Iowa State University, Ames, IA 50011

The Taos Range (Fig. 1.14) exposes a section of the Proterozoic middle crust that includes some of the highest grade metamorphic rocks in New Mexico (~ 6-8 kb, 700°C) (Pedrick et al., 1998). Deformation, metamorphism, and geochronology data from middle crustal exposures here and elsewhere in northern New Mexico (Tusas, Picuris, Cimarron, Rio Mora and Rincon uplifts) have provided the framework for constructing a complicated, multi-phase Proterozoic regional tectonic history where an apparent ca. 1.65 Ga macroscopic geometry is thoroughly overprinted by a ca. 1.4 Ga thermal event (Williams et al., 1999).

Proterozoic rocks in northern New Mexico are dominated by felsic to mafic metavolcanic rocks (1.76 - 1.7 Ga) intruded by calcalkaline plutons (1.75 - 1.64 Ga) (Bowring et al., 1984), interpreted to be juvenile island arcs that were accreted onto the Laurentian margin (Karlstrom & Bowring, 1988; Aleinikoff et al., 1993). Overlying this basement complex is the ca. 1.7 Ga Hondo Group, a thick sequence of quartzites and pelites (Bauer and Williams, 1989), that in the Taos Range are complexly interleaved with older basement rocks and younger 1.7 - 1.64 Ga granitoids.

The Tertiary Questa caldera divides the Taos Range into distinctive northern and southern halves. The higher-temperature northern Taos Range is dominated by amphibolite to upper-amphibolite facies supracrustal rocks (quartzite, pelitic gneiss, amphibolite) and 1.7 – 1.64 Ga calcalkaline plutons. Supracrustal rocks in the southern Taos Range are mainly metavolcanic rocks (with some metasedimentary rocks along the western edge of the range) of greenschist to amphibolite facies that are intruded by 1.75 - 1.7 Ga plutonic rocks. The earliest foliations observed throughout the range are bedding-parallel layers of kyanite (S_1) that are folded into F_2 intrafolial isoclinal-to-tight folds to produce the main S_2 fabric. All supracrustal and plutonic rocks have a strong S_2 foliation. S_2 is folded by upright northeast-trending F_3 folds. In the southern Taos Range, S_2 varies from a northeast-striking, variably dipping fabric in the southernmost areas, to a nearly east-west, steeply dipping fabric with an east-west plunging lineation (L_2) near Red River Canyon. In the northern Taos Range, S_2 strikes north to northeast, dips moderately to the west, and has a down-dip mineral lineation. High-grade supracrustal rocks sandwiched between 1.68-1.64 Ga gneiss packages, as well as the tectonized contacts themselves, record top-to-the-east/southeast shearing and indicate contacts are east-directed ductile thrusts parallel to S_2. Ductilely and cataclastically deformed feldspars, mica fish, and quartz mylonites indicate fabric development parallel to S_2 and shearing over a range of temperatures. Timing of S_2 development is constrained by the age of the youngest granitic gneiss (1.64 Ga) and weakly deformed 1.42 Ga *in situ* melts that cross-cut S_2 but exhibit top-to-the-east shearing (Pedrick et al., 1998).

A polyphase metamorphic history is recorded in quartz-rich rocks in both halves of the range, where kyanite is an early phase (M_1), sillimanite (M_2) is axial planar to isoclinally folded kyanite and defines S_2, and Mn-andalusite/andalusite and chloritoid are late phases (M_3). In the northern Taos Range, M_2 is characterized by sillimanite + K-feldspar in pelitic gneisses. Segregations or pods of sillimanite + quartz in pelitic gneisses (Cedro Canyon) and calc-silicates in amphibolites (Latir Canyon) are parallel to L_2 and S_2 and record top-to-the-east/southeast shearing. "Triple-point" rocks with kyanite, sillimanite, and Mn-andalusite are found in Cedro Canyon, but are not in equilibrium as kyanite is clearly early and Mn-andalusite directly replaces kyanite and sillimanite. Garnet-biotite thermometry and garnet-sillimanite-plagioclase barometry on pelitic gneisses in the northern Taos Range yield peak P-T estimates of 650-700°C and 6-8 kb, consistent with peak M_2 petrogenetic grid constraints. Texturally late Mn-andalusite in quartzite and chloritoid in quartzite and pelitic gneiss suggest M_3 conditions of ≤ 4 kb, 475-550°C.

Peak M_2 mineral assemblages in pelitic schists in the southern Taos Range include staurolite + sillimanite in Columbine Canyon and staurolite + kyanite further south in San Cristobal. Sillimanite is present in San Cristobal quartzite, but only when biotite is also present. The lack of biotite in San Cristobal schist may have prevented sillimanite from nucleating in these rocks as they passed through the sillimanite stability field. Textural observations and petrogenetic grid constraints suggest maximum P-T conditions in San Cristobal schist slightly below the intersection of the kyanite-sillimanite boundary with the staurolite breakdown reaction, while maximum conditions in Columbine were likely at this reaction boundary (ca. 6 kb, 620°C). Garnet-biotite thermometry and garnet-hornblende-plagioclase and garnet-plagioclase-biotite barometry yield maximum P-T estimates of 6 kb, ≥ 550°C for the southern Taos Range. Late chloritoid and andalusite in San Cristobal schist record M_3 conditions of ≤ 3.75 kb, ≤ 550°C.

Peak M_2 pressures probably do not differ all that greatly across the range, but peak temperatures vary by at least 100°C, decreasing from north to south. Consequently, although clockwise P-T paths for different halves of the range are always defined by early kyanite (M_1), peak sillimanite (M_2), and late andalusite (M_3), they are nested together, reflecting the differences in thermal history across the range. The hottest rocks in the northern Taos Range are sandwiched between 1.68-1.64 Ga granitic gneisses, suggesting that the high temperature metamorphism (M_2) may have been synchronous with thrusting of hot granitic sheets over and under supracrustal rocks. Granitic rocks of this age are lacking in the southern Taos Range, which may explain why M_2 temperatures are not as high there. However, *in situ* melts in the northern Taos Range imply temperatures greater than 600ºC at 1.42 Ga, so M_2 may be associated with this thermal event and not 1.65 Ga tectonism. Metamorphic mineral ages of ca. 1.4 Ga support this interpretation. Metamorphic zircon and titanite from amphibolite in Latir Canyon have U-Pb ages of 1.42 Ga and 1.38 Ga, respectively (Bowring and Karlstrom, 1994). Hornblende from amphibolite has $^{40}Ar/^{39}Ar$ cooling ages that range from 1.29-1.37 Ga (Karlstrom et al., 1997), with the youngest ages coming from

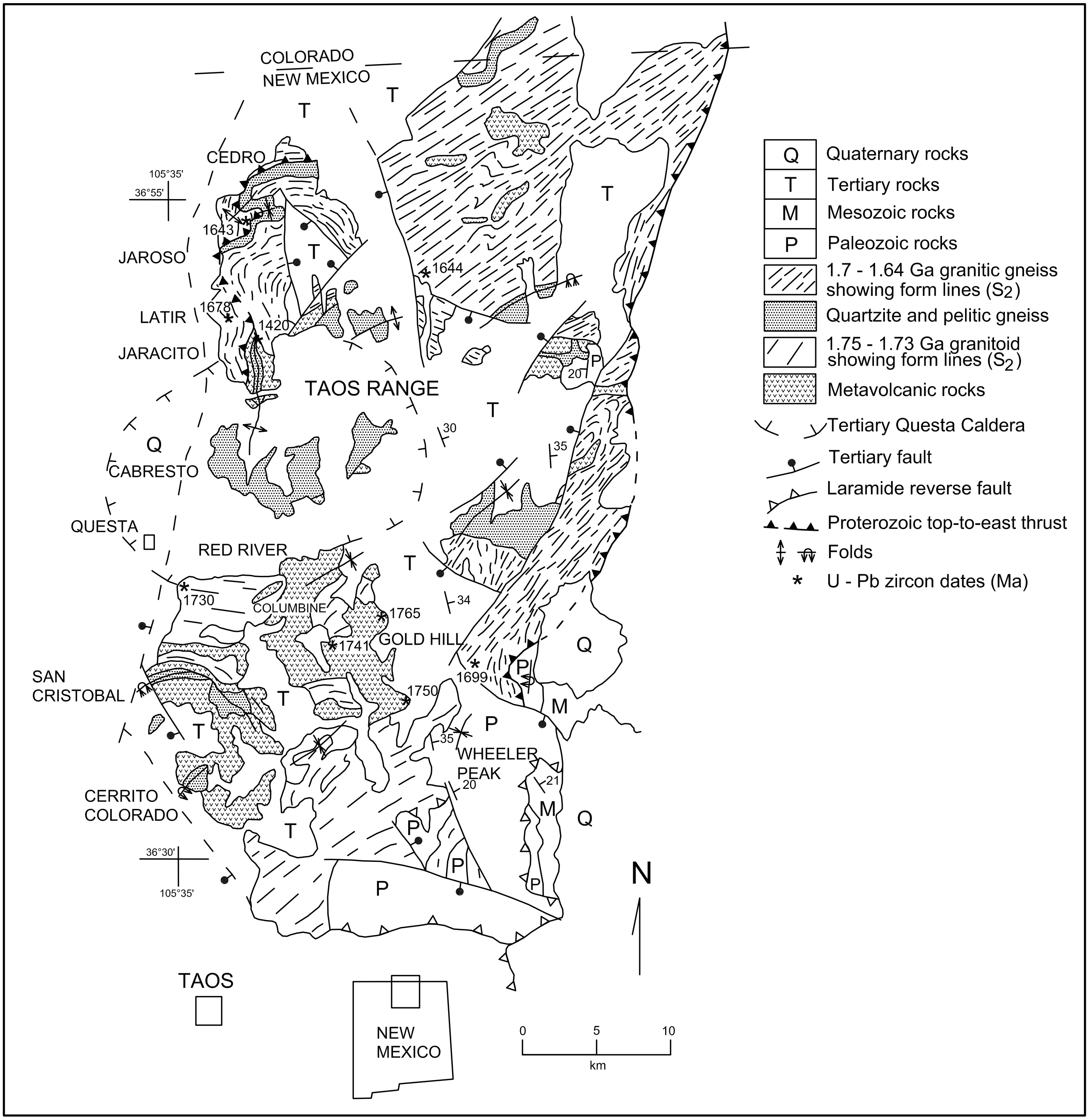

FIGURE 1.14. Generalized Proterozoic geology of the Taos Range (after Pedrick et al., 1998). Geochronology shown on the map is from Bowring et al. (1984), Bowring, unpub. data in Lipman and Reed (1989), and Bowring and Karlstrom (1994).

the hotter northern Taos Range. These minerals are aligned in S_2, suggesting reactivation of S_2 or an overprinting of earlier fabrics at 1.42 Ga. M_3 assemblages record decompression to ca. 4 kb during or after the 1.42 Ga thermal event. F_3 folds might represent minor deformation at this time, but much greater deformation associated with M_3 has been documented regionally in the Picuris Mountains (Williams et al., 1999).

It is clear from work in the Taos Range and other northern New Mexico Proterozoic uplifts that the ca. 1.4 Ga event affected the entire region, heating the middle crust to temperatures in excess of 550ºC (Williams et al., 1999), even in areas where there are no 1.4 Ga plutons, such as the Taos Range. New mineral growth or resetting of existing minerals aligned in S_2, as well as annealing of earlier fabrics at 1.4 Ga, obscures the nature of older fabrics that may have developed during arc accretion and assembly at 1.65 Ga. Williams et al. (1999) interpreted field geometries across the Proterozoic uplifts in northern New Mexico to have been established at 1.65 Ga, but reactivated and modified at 1.4

Ga. The extensive regional impact of the 1.4 Ga event suggests that mantle underplating may have been involved. Recent seismic work has identified a variable-thickness, high-velocity layer at the base of the crust along the length of the southern Rocky Mountains, interpreted to be the result of underplating that may have occurred at 1.7, 1.4 and 1.1 Ga (CD-ROM Working Group, 2002).

REFERENCES

Aleinikoff, J. N., Reed, J. C. and Wooden, J. L., 1993: Lead isotopic evidence for the origin of Paleo- and Mesoproterozoic rocks of the Colorado Province, U.S.A.: Precambrian Research, v. 63, p. 97-122.

Bauer, P. W. and Williams, M. L., 1989, Stratigraphic nomenclature of Proterozoic rocks, northern New Mexico – revisions, redefinitions, and formalization: New Mexico Geology, v. 11, p. 45-52.

Bowring, S. A. and Karlstrom, K. E., 1994, Thermochronologic constraints on Proterozoic lithospheric evolution, southwestern U.S.: Geological Society of America Abstracts with Programs, v. 26, p. 6.

Bowring, S. A., Reed, J. C. and Condie, K. C., 1984, U-Pb geochronology of Proterozoic volcanic and plutonic rocks, Sangre de Cristo Mtns., NM: Geological society of America Abstracts with Programs, v. 16, p. 216.

CD-ROM Working Group, 2002, Structure and evolution of the lithosphere beneath the Rocky Mountains: Initial Results from the CD-ROM Experiment: GSA Today, v. 12, no. 3, p. 4-10.

Karlstrom, K. E. and Bowring, S. A., 1988, Early Proterozoic assembly of tectonostratigraphic terranes in southwestern North America: Journal of Geology, v. 96, p. 561-576.

Karlstrom, K. E., Dallmeyer, R. D. and Grambling, J. A., 1997. $^{40}Ar/^{39}Ar$ evidence for Mesoproterozoic regional metamorphism in northern New Mexico: implications for lithosphere evolution in the Southwest: The Journal of Geology, v. 205, p. 205-223.

Lipman, P. W. and Reed, J. C., 1989. Geologic map of the Latir volcanic field and adjacent areas, northern New Mexico: U.S. Geological Survey Map I-1907, 1:48,000.

Pedrick, J. N., Karlstrom, K. E. and Bowring, S. A., 1998, Reconciliation of conflicting tectonic models for Proterozoic rocks of northern New Mexico: Journal of Metamorphic Geology, v. 16, p. 687-707.

Williams, M. L., Karlstrom, K. E., Lanzirotti, A., Read, A. S., Bishop, J. L., Lombardi, C. E., Pedrick, J. N. and Wingstead, M. B., 1999, New Mexico middle-crustal cross sections: 1.65 Ga macroscopic geometry, 1.4 Ga thermal structure, and continued problems in understanding crustal evolution: Rocky Mountain Geology, v. 34, no. 1, p. 53-66.

Kelson and Bauer (2003). This south-sloping terrace overlies the Servilleta Basalt, and likely reflects aggradation on the Taos Plateau prior to the down-cutting that later formed the Rio Grande Gorge. Kelson (1986) correlated this terrace with alluvial-fan deposits in the southern Taos Plateau that contain an ash dated at 1.27 ± 0.02 Ma (Bauer et al., 1999a). **0.2**

76.3 The road descends here from the Qf1 fan surface onto a fluvial terrace inset into the Qf1 deposits. This Qt2 terrace is associated with a broad wind gap on the southern side of the Rio Hondo valley; the small hill north of the road (and south of the valley rim) is a remnant of the Qf1 fan surface.

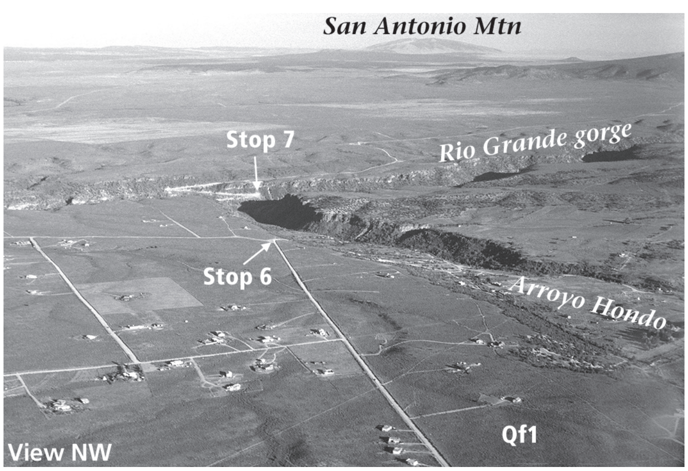

FIGURE 1.15. Aerial view northwestward of the confluence of the Rio Grande and Rio Hondo, showing the locations of STOPS 6 and 7. A series of low-relief Pliocene volcanoes populate the Taos Plateau, with the ca. 3 Ma San Antonio Mountain stratovolcano in the distance.

Both the Qt2 and Qf1 surfaces overlie the Servilleta Basalt, and pre-date the formation of the Rio Grande gorge. **1.1**

77.4 STOP 6. Rio Hondo Drainage Overlook.

[16] Pullout on the left side of the road and park.

This is an overlook into the Rio Hondo drainage to discuss the complex history of river terrace evolution along the Rio Hondo. **1.1**

The breathtaking views of the Rio Grande gorge and Arroyo Hondo (Fig. 1.16) are a result of 120 m of Quaternary incision into the Servilleta Basalt underlying the Taos Plateau. This incision has also resulted in long-term changes along the tributaries that drain the Taos Plateau and the southern Sangre de Cristo Mountains. The primary tributaries are the Rio Hondo and Rio Pueblo de Taos, which flow into the Rio Grande 10-to-15 km west of the mountain front and exhibit distinct responses to the lowering of base level. The entire sequence of six Rio Hondo strath terraces is preserved in this area, with each terrace remnant located lower and farther east from the next higher, older terrace. Each of the terraces is associated with thin (<3 m) alluvial gravel deposited on a strath surface usually cut on the Servilleta Basalt. The intersection of the basalt and the floodplain at the time of terrace formation has migrated eastward through time, as incision along the Rio Hondo progressed.

The longitudinal profiles of terraces below the Sangre de Cristo mountain front are sub-parallel to the straight, steep (23 m/km) channel gradient of the present-day Rio Hondo. The terrace profiles also grade smoothly to the Rio Grande, and lack substantial profile knickpoints. Above the mountain front, the Rio Hondo drainage basin is underlain by resistant granite, gneiss, and rhyolite. Present-day unit discharges (normalized

FIGURE 1.16. Panoramic view northeastward of the Arroyo Hondo valley from STOP 6. The valley preserves parts of six distinct strath terraces that record a complex history of incision and stream capture.

by drainage area) on Rio Hondo are high and estimates of bed shear stress and stream power suggest that the river can transport the majority of channel bed material at bankfull discharge. The presence of strath terraces suggests that Rio Hondo has had sufficient stream power through geologic time to maintain sediment transport and to incise into underlying basalt in response to base-level lowering imposed by incision of the Rio Grande. Lithologically controlled high discharge, stream power, and sediment transport rates acting over the past 1 Ma or so apparently have enabled the Rio Hondo to keep pace with continued incision of the Rio Grande.

In contrast, the broad Rio Pueblo de Taos valley contains fewer fluvial terraces, and there is less relief between these terraces than those in the Rio Hondo valley. The long-profile of the Rio Pueblo de Taos does not grade to the Rio Grande; instead it has a shallow gradient across the Taos Plateau until it encounters basalt outcrops about 4 km upstream of the Rio Grande, and then drops steeply to the Rio Grande confluence. The Rio Pueblo de Taos drainage basin contains several tributaries that are underlain primarily by Pennsylvanian sandstone and shale above the Sangre de Cristo mountain front. Present-day unit discharges on these tributaries are comparatively low, and estimates of bed shear stress and stream power are lower in channels draining sedimentary rocks than in those draining crystalline rocks.

A lack of sustained high discharge on the streams draining sedimentary rocks suggests that the total amounts of bedload material transported are relatively low. It is likely that the lithologically controlled discharge characteristics along tributaries within the Rio Pueblo de Taos drainage area, acting over geologic time, have had a strong influence on the ability of the lower Rio Pueblo de Taos to incise into the basalt close to the Rio Grande. Thus, the response of Rio Pueblo de Taos to incision along the master Rio Grande has been quite different than along the Rio Hondo, and likely is related to the rock types and consequent discharge characteristics in the tributary headwaters.

End of Stop 6. Return to vehicles and continue on gravel road down into Arroyo Hondo towards the Rio Grande.

77.7 Borrow pit on right exposes gravel of the Blueberry Hill deposits of Bauer and Kelson (2001) and Kelson and Bauer (2003) and the "Basin Fill deposits" of Kelson (1986). These deposits have smaller clast sizes and much greater oxidation than the younger alluvial-fan (Qf1) and fluvial (Qt2 to Qt7) deposits mapped on the Taos Plateau. The source area for these deposits probably is the ancestral Red River drainage, which at that time was the headwaters of the Rio Grande (Wells et al., 1987). **0.3**

77.8 [17] **Bear left** at the fork and follow the Rio Hondo to the confluence with the Rio Grande. We are descending through the stack of Servilleta Basalt flows. **0.1**

78.2 A thick section of sand and gravel between basalts exposed in left roadcut. **0.4**

78.4 The road descends into the Rio Grande gorge along the Rio Hondo through a thick silicic alkalic basalt flow from an unknown vent area (discussed at STOP 7). Similar flows are exposed elsewhere along the Rio Grande gorge and represent a rare basalt type in the Taos Plateau volcanic field. Notice differences in texture and fracture patterns between these rocks and the more mafic overlying flows of the Servilleta Basalt. **0.2**

78.7 Crossing the Rio Hondo. The silicic alkalic basalt cliff to the right, known as "John's Wall," is popular with local rock climbers. **0.3**

78.9 [18] **Cross the Rio Grande on the John Dunn Bridge and turn left.** The steeply dipping, west-down Dunn fault parallels the river here. Originally, the John Dunn Bridge was a toll bridge built and operated by "Long John" Dunn who ran a passenger stage business between Taos and the rail stations at Taos Junction and Servilleta. The name Servilleta originally applied to Servilleta Plaza, a small village just west of the Rio Arriba county line. When the D&RG railroad was built, it transferred the name to a siding that once existed 10 miles south of Tres Piedras (Julyan, 1996). Just past the bridge, baked sediments are visible beneath the basalt flow at road level (Fig. 1.17). This is the put-in for the popular expert whitewater run of the lower Taos Box. Many commercial river outfitters run rafting trips through the box during spring and summer months (Fig. 1.18). **0.2**

79.1 Trailhead to Black Rock hot spring is at first switchback; this spring and the Manby hot spring (Fig. 1.19) downstream about 2 miles (3.5 km) lie along the Dunn fault that runs nearly parallel to the river. The fault crosses the road just above this switchback and again above the second switchback. Black Rock hot spring is one of the most scenic outside the Jemez Mountains. The spring is right along the river and remains at about 36°C (97°F) except when the river is high enough to flood it. The spring discharges approximately 80 l/min (21 gal/min or 0.05 cfs). A somewhat frightening small vapor cave in basalt talus can be entered just uphill from the springs. Manby hot springs consist of three independent pools with discharges of 314 l/min (83 gal/min or 0.18 cfs), 38 l/min (10 gal/min or 0.02 cfs), and 61 l/min (16 gal/min or 0.04 cfs). The water averages around 38°C (100°F), but the lower pool tends to be cooler due to mixing with river water. These springs were once owned by Arthur R. Manby, an English mining engineer and controversial local figure who was found decapitated in his home in 1929 (Julyan, 1996). **0.2**

79.2 Ascending past thick gravels between basalt flows. **0.1**

79.5 Bright red/yellow baked zone in roadcut on the right. **0.3**

79.8 [19] STOP 7. Confluence Rio Grande Rio Hondo. Turn right into pullout. (after the steep switchbacks). Here we visit an overlook of the confluence (Fig. 1.20) and discuss the volcanic features and faults visible in the canyon walls. **0.3**

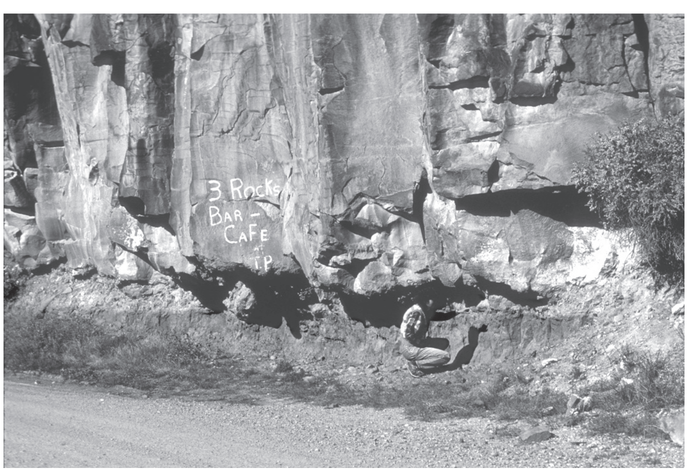

FIGURE 1.17. A zone of red-baked sediment is visible below this Servilleta basalt flow on the west side of the Dunn Bridge along the Rio Grande. This common alteration scenario is found over much of the Taos Plateau, and suggests that wetlands and lakes were probably common here during the Pliocene.

FIGURE 1.18. Swim anyone? A plunge into the Rio Grande through the 15-mi Class IV whitewater section of the Lower Taos Box can provide a chilling perspective on the 31 ft/mi gradient through this section of the canyon.

Dunn fault:
The Rio Grande at this locality roughly parallels the trace of the steeply dipping Dunn fault (Fig. 1.21) that displaces the Servilleta Basalt about 35 m, with a east-down sense of movement (Peterson, 1981; Machette and Personius, 1984). The fault crosses the west side of the gorge at approximately the location of the lowermost switchback and climbs out of the gorge immediately behind this vantage point (Fig. 1.21). To the south, approximately where the Rio Grande disappears from view to the west, the fault climbs the eastern gorge wall marked by a small deflection in the topography at the skyline and a talus fan deposit in the gorge. At river level, hot springs occur on both sides of the Rio Grande along the fault trace. The Black Rock hot spring is just downstream from the first switchback and the Manby hot springs are about a mile further downstream. Interestingly, the Rio Grande gorge in this area consists of several relatively straight sections that coincide with several of these linear fault traces (Fig. 1.22), suggesting that the incision of the Rio Grande may have occurred along zones of fractured basalt related to these discontinuous faults.

The Dunn fault is one of a number of east-down normal faults accommodating extensional basin sedimentation in the Taos graben. The north-striking fault is mapped on the basis of stratigraphic separation or geomorphic expression for about 3 km. Along the southern projection of the Dunn fault and within and adjacent to the Rio Grande Gorge, Kelson and Bauer (1998, 2003) mapped several discontinuous north-striking faults that displace the Servilleta Basalt with west- and east-down vertical separations. These faults parallel the Los Cordovas fault system to the east, and may be part of a broad zone of distributed deformation underlying the Taos Plateau. At the southern end of the Taos Plateau, a similar north-striking, east-down fault branches from the northeast-striking Embudo fault. Only locally do these

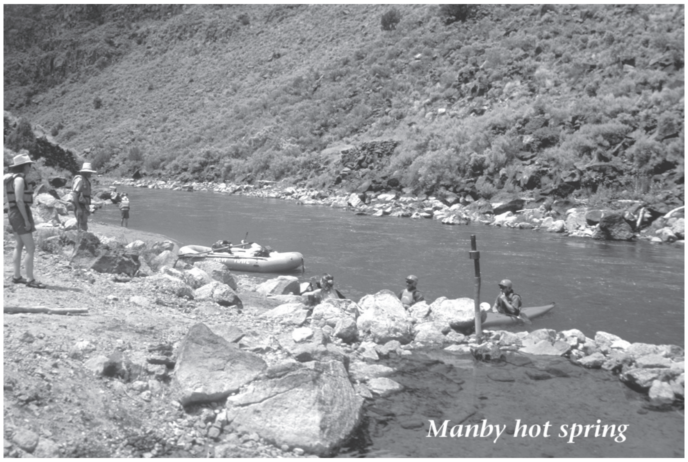

FIGURE 1.19. Riverside view of the lower pool at Manby hot springs. The 38°C (100°F) water discharges near the east canyon wall, and is probably related to the Dunn fault, which crops out just to the east. A steep foot trail leads to the spring from the eastern rim of the gorge.

faults displace the ancestral Rio Grande gravel deposits that overlie the Servilleta Basalt.

Silicic Alkakic Basalt:

The term "silicic alkalic basalt" was originally used by Lipman and Mehnert (1975) in reference to basalts of the southern Rocky Mountain region that are compositionally distinct from olivine tholeiites and alkali-olivine basalts. On the Taos Plateau these rocks are relatively rare and are characterized by 50-53 wt% SiO_2, and higher total alkalies and incompatible element concentrations (LREE, Rb, Nb, Zr, Th and U) than the more common Servilleta tholeiites. Phenocrysts typically include olivine and variable amounts of complexly zoned plagioclase in an intergranular groundmass matrix. Silicic alkalic basalt flows, such as the sequence exposed in the gorge below (Fig. 1.20), are variably thickened relative to tholeiites and are characterized by brecciated aa margins and often develop radial joint patterns in the massive interiors of flow lobes. Although this rock type is considered a volumetrically minor constituent of the Taos Plateau volcanic field it is the regionally dominant basalt type associated with Rio Grande rifting and constitutes the preponderance of mafic lavas erupted during the Oligocene and Miocene rifting events. The silicic alkalic basalt flows exposed here are presumed to have a local, but undetermined, source area.

Timing of faulting, sedimentation, volcanism:

The Taos graben was mostly formed by the time the flows of the lower Servilleta Basalt erupted ca. 4.8 Ma. On the Taos Plateau, the Rio Grande was superposed on the plateau after eruption of the youngest flows of the Servilleta Basalt (ca. 3 Ma), and began to rapidly entrench upon integration of the river system at approximately 0.5 Ma (Wells et al., 1987). Although most of the high-angle faults on the plateau did not cause thickening or thinning of volcanic flows across the faults, evidence exists for active rift faulting during eruptions of Servilleta Basalt and when the interlayered basin fill sediments were accumulating (Peterson, 1981; Dungan et al., 1984). Dungan et al. (1984) reported a 17 m (56 ft) thicker sedimentary sequence east of the fault, between flows of the upper and middle Servilleta Basalt, and attributed that to active faulting and basin sedimentation during eruption of the basalts.

Besides having thicker sedimentary sections on the downthrown side of the Dunn fault, the basalt flows on the downthrown side all have baked zones (Fig. 1.17) indicative of marshy land surfaces. The upthrown sides have no baked zones. The magnetic polarity of the basalts changes from reverse below the thick gravel layer to normal above it (Ozima et al., 1967).

FIGURE 1.20. View east from STOP 7 of the confluence of the Rio Grande and Rio Hondo. The silicic alkalic basalt is well exposed at road level. The small quarry in gravels above the alkalic basalt is an abandoned hydraulic gold mining operation. These gravels thin noticeably downstream from the confluence.

FIGURE 1.21. View south, downstream of the Rio Grande gorge from STOP 7. Although its trace is buried along the river valley, the Dunn fault leaves the canyon just to the south, where Servilleta Basalt is down-dropped east along the steep fault.

The upper and middle flow-packages of the Servilleta Basalt are substantially thinner here than to the south (see STOP 8). The thin sequence of tholeiites are likely the result of the topographic shielding effect imposed on east-flowing lavas of the Servilleta Basalt by the topographic barriers at Timber Mountain, Cerro Montoso, and Cerros de los Taoses.

Placer mining:

Placer gold and silver exist in the gravels of the ancestral Rio Grande and tributaries that are eroded rocks within the mining districts of the Taos Range. Small placer mining operations have attempted to recover this gold since Spanish colonization. According to Schilling (1960), gravels along the Rio Hondo (Fig. 1.20) were prospected with shallow shafts. A floating dredge was built ~18 miles downstream near Taos Junction bridge but only operated for a few weeks before operations were halted by the abundance of large basalt talus blocks in the riverbed. The excavated yellowish coarse gravels visible from this stop on the opposite side of the gorge and just above the confluence of the Rio Hondo were a prospect for a gold mining operation that used an aqueduct for hydraulic mining. These claims, surveyed in 1892 and 1893, were never patented (R. Eveleth, personal commun., 2004).

End of Stop 7. Return to vehicles and continue drive up onto the west rim of the gorge.

80.1 Cattle guard; fault to the west; scarp is parallel to the road. **0.3**

80.8 [20] **Arrive at top of canyon rim. Stay straight at intersection. 0.7**

80.9 Descending into gorge-parallel asymmetric valley that may be a strand of the Dunn fault. The fault is difficult to follow to the south where it is covered by ancestral Rio Grande gravels (Fig. 1.23). **0.1**

83.1 Basalt exposed along west side of another asymmetric gorge-parallel valley. **2.2**

83.7 Stay left on main dirt road, and then cross under powerlines. **0.6**

84.6 [21] **Turn left onto US-64**. Cerro de los Taoses volcanic center is at 12:00 before the bend in road. **0.9**

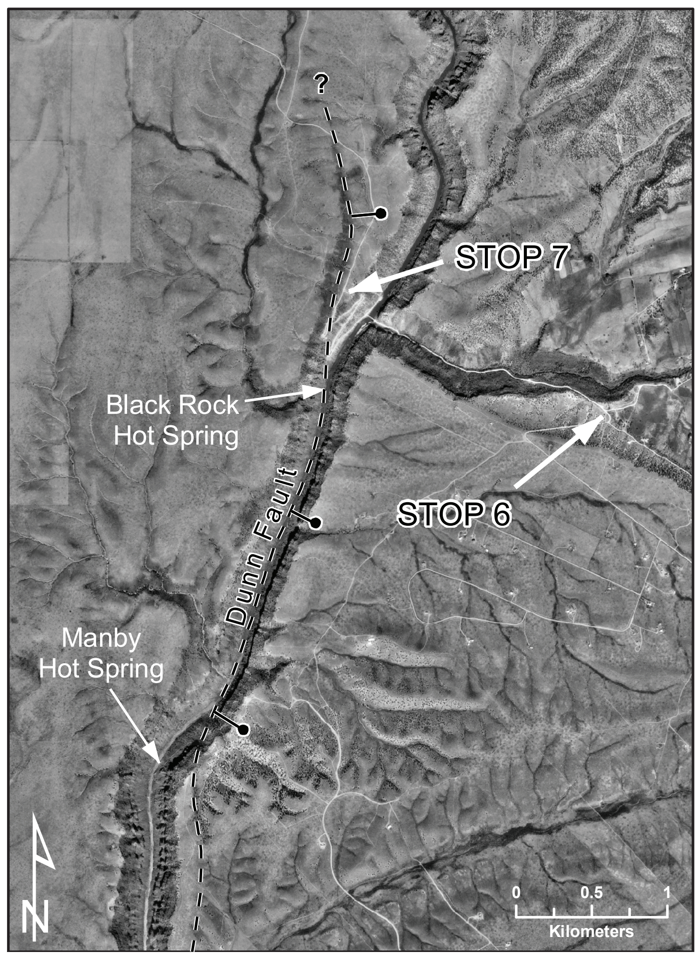

FIGURE 1.22. USGS orthophoto image from 1997 showing the trace of the Dunn fault and the hot springs that probably represent deep geothermal flow systems that utilize the fault zone. Location of the fault is from Dungan et al. (1984) and Kelson and Bauer (2003).

SIDEBAR 1.3 - Earthship architecture

These homes are part of The Greater World Earthship Community, a subdivision intent on practicing sustainable living principles. The passive solar homes, with walls made principally from dirt rammed into tires or from other recycled materials, are entirely off the electric grid and use photovoltaic panels for power. Off-site water and electricity are specifically banned by community covenants. Water is collected from rain-catchment rooftops, stored in cisterns, and graywater is recycled for various non-potable uses. A backup community well is in place for times of severe drought. Residents own their lots as well as a stake in community parkland and facilities.

Despite (because of?) their utopian ideals, this community has caused considerable controversy in Taos. In 1997, the county sued architect Michael Reynolds, the originator of the Earthship idea and developer of the subdivision, for violation of the State Subdivision Act because he did not apply for a subdivision permit for the development. The county was concerned that the community would not have sufficient infrastructure in place, like roads and schools, leading to an eventual negative impact on county taxpayers. The Taos County Planning Board subsequently filed injunctions against further construction. Mr. Reynolds claimed that Earthships provide their own infrastructure and that, at the time, he was selling 'memberships' in the community and not land. To resolve the standoff, Mr. Reynolds submitted a subdivision application in 1998. However, this was not the end of the controversy. To avoid pending lawsuits regarding life-safety issues with these and other structures, disgruntled customers, and apparently questionable business practices, Michael Reynolds permanently surrendered his NM State-issued Architect and Contractor's licenses to the NM Attorney General on March 17, 2000.

Regardless of the issues surrounding the Greater World Earthship Community, residents of Taos County continue to innovate using solar technology and architecture as well as alternative building practices to take advantage of the almost-always sunny skies. Taos has a solar-powered radio station, KTAO 101.9 FM, and hosts the annual Taos Solar Music Festival, sponsored by the New Mexico Solar Energy Association, which highlights solar technologies for residential use

89.2 Passing the Wolf Springs Ranch on right. Notice the Earthship homes on left of highway (Fig. 1.24). (See sidebar 1.3) **4.6**

89.6 The gravel mining operations north of US-64 are extracting materials deposited by the ancestral Rio Grande (unit Qt1rg of Kelson and Bauer, 2003). **0.4**

90.2 [22] **Turn right** onto unmarked dirt road before US-64 bends east. **0.6**

92.1 Old log cabins on right served as 'Mission Control' during part of the Apollo 15 exercises along the Rio Grande Gorge conducted by Bill Muehlberger in the 1960s. **1.9**

93.0 [23] **Turn left onto unmarked dirt road** that heads east near the colorful old school bus that has been converted to a home. Respect any and all private property signs in this area. **0.9**

94.2 [24] **Before plunging 600 feet into the gorge, turn right onto the rim-parallel road**. **1.2**

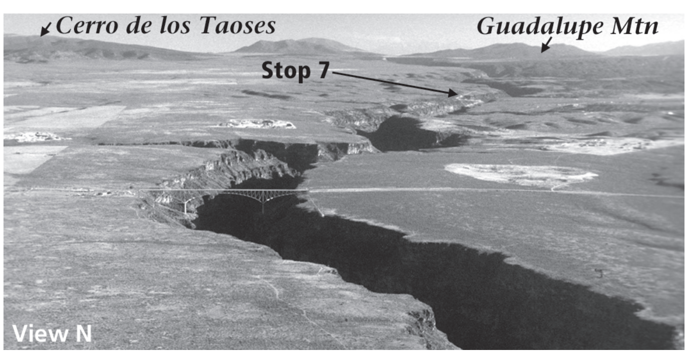

FIGURE 1.23. Aerial view northward of the Rio Grande gorge and Gorge Bridge with the trace of the Dunn fault visible in the distance near STOP 7. The surface expression of the fault is absent north of the bridge, due to the extensive cover provided by Quaternary gravels. Numerous gravel quarries are developed in the ancestral Rio Grande gravel deposits, which consist of well-sorted, rounded clasts of predominantly mid-Tertiary volcanic rocks derived from volcanic terrains to the north. Several Pliocene volcanoes are silouetted on the skyline.

FIGURE 1.24. Earthship homes were popularized by actor Dennis Weaver, whose beautiful and efficient home in Ridgway, Colorado incorporated used tires, aluminum cans, and other recycled materials in its structure. Earthships, such as this Taos County home, are passive solar designs that use thermal mass to regulate seasonal heating and cooling requirements. Electricity is supplied by photovoltaic panels.

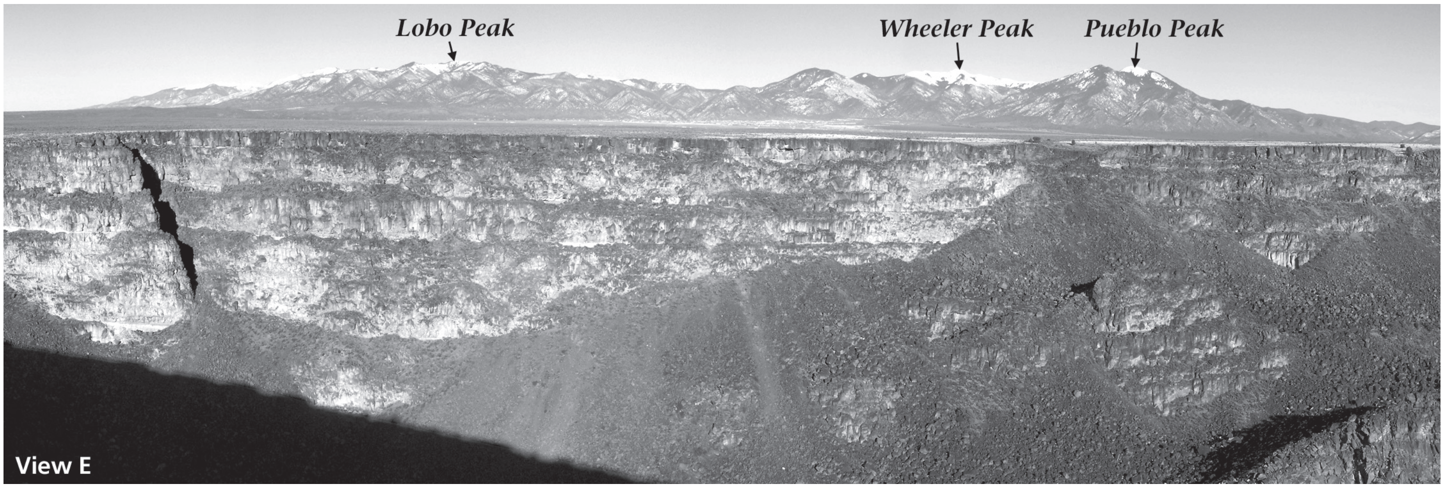

FIGURE 1.25. Panoramic view of east Rio Grande gorge wall and Sangre de Cristo Mountains from STOP 8. This view is along the axis of the Gorge arch. Flow-packages of the lower, middle, and upper Servilleta Basalt are visible on the canyon wall, each separated by a layer of basin-fill sediment. The highest basalt flow on the rim is believed to exist only here, and is an erosional remnant of a flow that might have erupted east of the gorge.

94.5 STOP 8. Rio Grande Gorge Rim Overlook.
[25] Park and walk to rim overlook.

Here we will discuss gorge stratigraphy (Fig. 1.25), Rio Grande incision history, landslides, the Gorge arch, subsurface basalt geometry, and hydrogeology of the plateau **0.3**

Gorge morphology:

We are standing at a fascinating, but poorly understood, geomorphic boundary of the southern Taos Plateau. Several geomorphic changes intersect at this location. The northeast-trending Gorge arch intersects the Rio Grande gorge here. The gorge changes from a narrow (245 m wide at rim), steep canyon to the north to a broad (750 m wide at rim), less steep canyon to the south and this transition zone is characterized by an eastward jog of the river (Fig. 1.26). Correspondingly, the northern reach generally lacks large landslides, whereas the southern reach contains continuous back-rotated landslide blocks (toreva blocks, Fig. 1.27). Presumably, the variations in width, steepness, and landslide cover reflect a dramatic change from thin sediment fill between basalt flows to the north, to thick sediment fill between basalt flows to the south. Clearly, the interplay between Pliocene volcanism and sedimentation varied considerably north and south of here, perhaps due to activity on the Pliocene alluvial fans sourced in the Sangre de Cristo Mountains.

Gorge stratigraphy:

The Rio Grande gorge at this stop cuts through one of the thickest sequences of Servilleta Basalt in the Taos Plateau volcanic field. This is the essentially the same stratigraphic sequence exposed at the high bridge crossing (Fig. 1.28), both sections representing what may be considered "type" sections for the Servilleta Basalt (Lipman and Mehnert, 1979; Peterson, 1981; Dungan et. al., 1984). The Servilleta Basalt is volumetrically the dominant lithology of the Taos Plateau volcanic field and may encompass as much as 200 km^3 of olivine tholeiite with an aerial extent of > 1500 km^2. The Servilleta Basalt has an asymmetric distribution and thickness across the San Luis Valley and the stratigraphic section here (Fig. 1.25 and cover) represents a very thick accumulation of approximately 180 m (590 ft.). Most of the basalts in the gorge at this stop are presumed to have erupted from the vents to the west although nothing precludes buried source areas to the east. Recent geologic mapping (Kelson and Bauer, 2003) and aeromagnetic data of the Taos region suggests the possibility of a buried vent near the Taos airport (see Grauch et al., 2004, this volume and Plate 5). Relative to the thick sedimentary interbeds observed in the gorge to the north at the Dunn bridge, the thin sedimentary interbeds in the vicinity of the Gorge Bridge reflect the decreasing influence of the Hondo alluvial fan. Additionally, the thickened basalt sequence indicates not only the lesser influence of prograding alluvial fan deposits but also the decreased impact from paleotopographic highlands of the intra-rift horst further north.

The upper, middle and lower flow-packages of the Servilleta Basalt each represent multiple coalesced flows and are readily distinguished here on the basis of thin sedimentary interbeds separating these three informal units of subequal thickness. The sedimentary interbeds were originally thought to represent time intervals significantly longer than the eruption intervals of the basalt members (Peterson, 1981; Dungan et al., 1984; Caffall and Brown, 1985). Recent $^{40}Ar/^{39}Ar$ dating by Appelt (1998) suggests this may only hold true for the flows of the lower Servilleta Basalt (4.8 to 4.65 Ma) with a short eruption interval. Ages for middle (4.35 to 3.92 Ma) and upper (3.72 to < 2.62 Ma) flows of the Servilleta Basalt encompass a significantly wider range than the intervening sedimentary deposits.

All of the lavas of the Servilleta Basalt form pahoehoe flows commonly characterized by diktytaxitic or intergranular groundmass textures and 5-15% phenocrysts of Fo_{83-80} olivine and rarely plagioclase (Dungan, 1987). Vertical and horizontal vesicle pipes are common in these flows with coarser grained groundmass. Dungan et al. (1986) demonstrated that major and trace element compositions within the basalts are well correllated . Increasing SiO_2 and K_2O is accompanied by increases in incompatible elements (Zr, Nb, Hf, Th, Rb, Ba, Sr, LREE) and

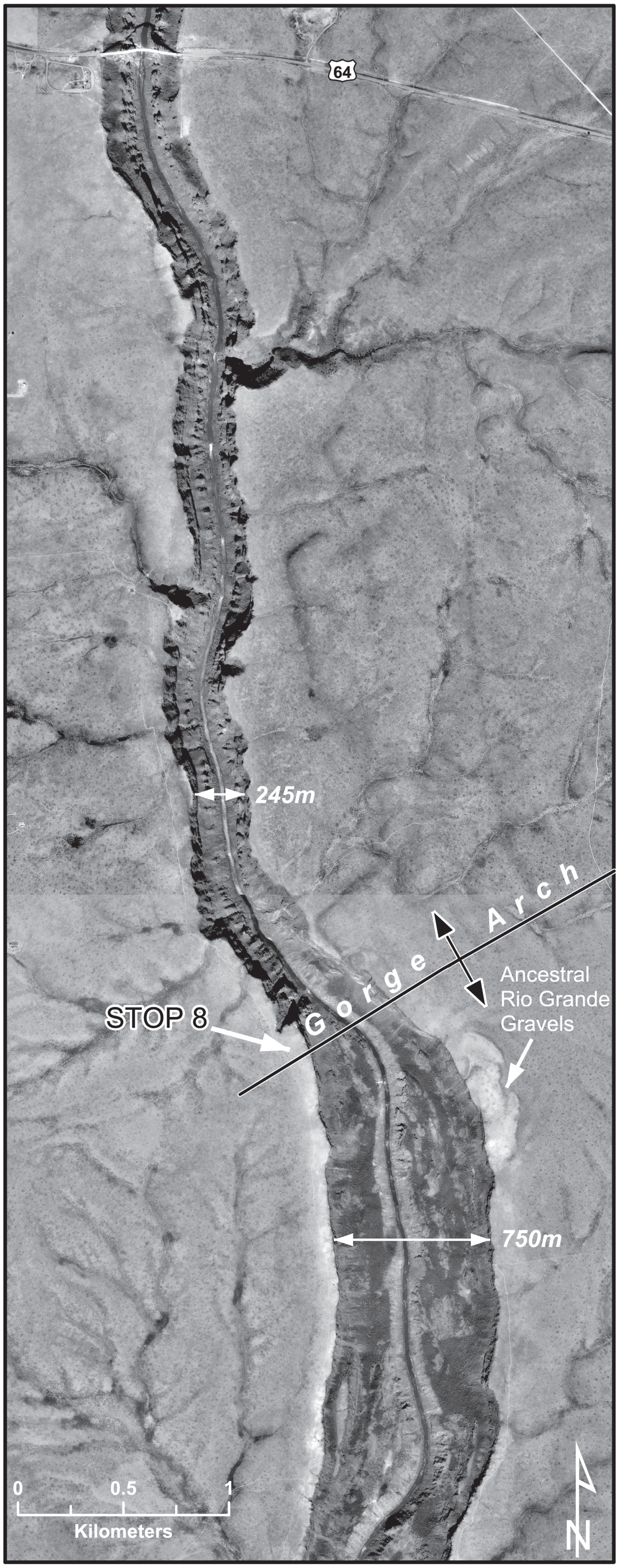

FIGURE 1.26. USGS orthophoto from 1997 of the central Rio Grande gorge region. The transition from a narrow, steep-sided gorge to a wide, moderately steep gorge with major landslides is coincident with the river-left bend and with the Gorge arch. Gorge Bridge is visible to north. Many of the large rapids (white areas) are also visible in the Rio Grande.

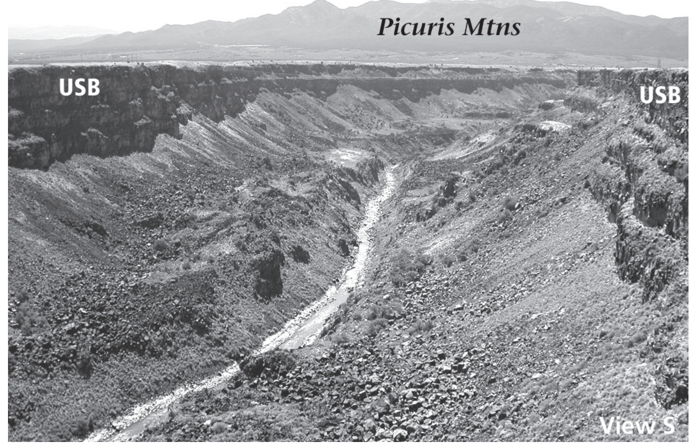

FIGURE 1.27. View downstream STOP 8. The Picuris Mountains are on the skyline. Here the gorge is about 750 m wide, and is mantled by Quaternary landslides, presumably due to the a thick sediment sequence below the cliff-forming upper flows of the Servilleta Basalt (USB).

decreases in Feo, TiO_2, CaO and MgO. The lavas with highest SiO_2, K_2O and incompatible elements are believed to be hybrid magmas, the result of mixing of mafic parent magmas and more evolved compositions (Dungan et. al., 1986; Dungan, 1987). These lavas are characteristic of the lower Servilleta basalt package. Low SiO_2 and K_2O compositions dominate the middle flows of the Servilleta Basalt; lavas from flows of the upper Servilleta Basalt span the entire compositional range observed for both underlying packages. This suggests that stratigraphic correlation based primarily on geochemical correlation can be problematic, especially in drill hole data.

River incision history:

Recent detailed geologic mapping of the area adjacent to the Rio Grande gorge between Manby hot springs and Rio Pueblo de Taos (Kelson and Bauer, 1998; 2003, see Plate 6) provided new insights into the faulting and folding of the Taos Plateau and late Quaternary history of the Rio Grande. North of this stop, the Rio Grande gorge is flanked by remnants of two distinct, south-sloping fluvial terraces, Qt1rg and Qt2rg (Figs. 1.29 and 1.26). These terraces are correlative with the west-sloping Qf1 fan surface and the Qt2 terrace remnants, respectively, along the Rio Hondo (see Fig. 1.15) and the Rio Pueblo de Taos (and the area in between these drainages.). Near Manby hot springs (about 8 km north of here), the 20-m-thick Qt1rg deposits are more than 3 or 4 km wide, and overlie the uppermost flow of the Servilleta Basalt. However, only 2 km north of here, the Qt1rg deposits are much narrower (< 1 km maximum) and are inset into the basalt. Similarly, the Qt2rg deposits are broader and more extensive near Manby hot springs, but are preserved only as small remnants near this stop. Remnants of the Qt1rg and Qt2rg are not present along the gorge rim from this point south for about 1 km.

The gorge rim in this area is topographically high, perhaps as a result of tectonic deformation (the "Gorge Arch," Muehlberger, 1979) or the presence of previously undocumented

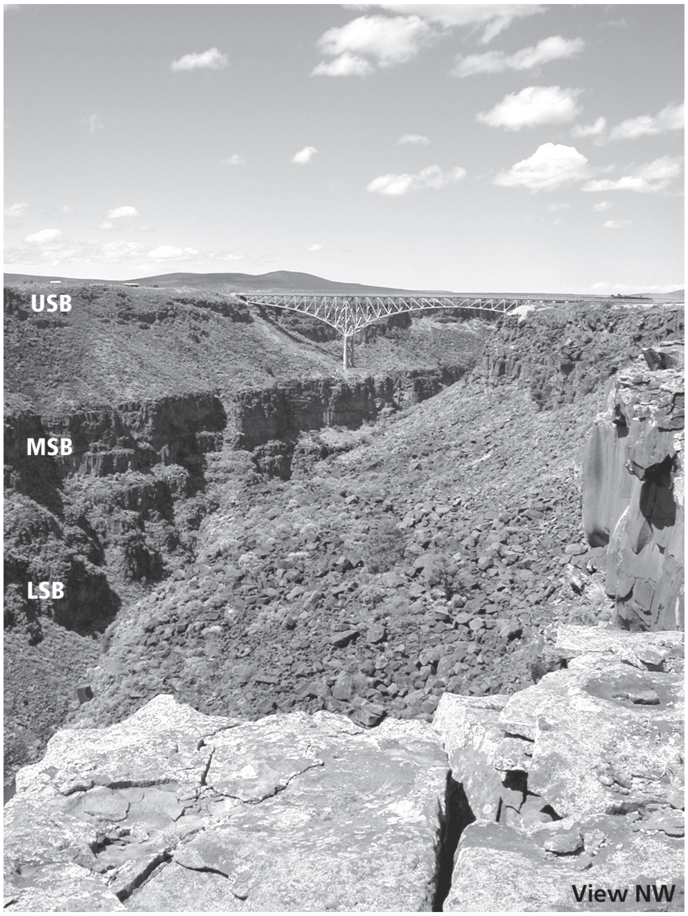

FIGURE 1.28. View north of the Rio Grande gorge and the Gorge Bridge from the east rim. The lower, middle, and upper flow-packages of the Servilleta Basalt (LSB, MSB, USB) are well exposed through this narrow and steep section of the gorge. The volcano on the skyline is the ca. 5 Ma Cerro de los Taoses.

FIGURE 1.29. Field photo of typical ancestral Rio Grande gravel exposed along the western rim of the gorge. The gravel consists primarily of moderately well sorted, rounded clasts of mid-Tertiary volcanic rocks, plus some Proterozoic rock types.

volcanic edifices east of the river (Kelson and Bauer, 2003). Downstream of the topographic high, the Qt1rg and Qt2rg terraces both re-appear, with the Qt1rg deposits fanning out from the gorge to be about 7 km wide near the Rio Pueblo de Taos. The Qt2rg surface is inset into the Qt1rg deposits to the south for about 13 km to the village of Pilar. Longitudinal profiles of both the Qt1rg and Qt2rg surfaces are parallel and exhibit no evidence of broad warping (Fig. 1.30). These relations suggest that if the northeast-trending Gorge arch is a tectonic feature, deformation pre-dates the Qt1rg terrace, which is estimated as about 1.27 Ma (Kelson and Bauer, 1998; 2003).

Gorge arch:

A number of very gentle, broad flexures were identified in the Taos area (Muehlberger, 1979; Peterson, 1981; Dungan et al., 1984; Personius and Machette, 1984). Their interpretations were based on drainage patterns and stream asymmetries on the Taos plateau. The Taos Airport lies along the axis of the Gorge arch (Fig. 1.31). The arch separates drainage that is deflected to the north from those that are deflected to the east. Asymmetric drainages in unconsolidated sediments suggest that uplift or warping along the axis of the arch is recent and probably still active. However, subtle dip changes in the basalt flows are imperceptible in the field. In the eastern Taos Plateau, Peterson (1981) identified seven domains of similarly oriented asymmetrical valleys, and suggested that the warping occurred after emplacement of the Servilleta Basalt. Interestingly, the two primary flexures, the Gorge arch and the syncline along the Rio Pueblo de Taos, are parallel to the Embudo fault zone, and bracket the deepest part of the Taos graben and Los Cordovas fault zone. The flexures are probably a surface manifestation of the complex subsurface fault geometry, but the precise relationships are unknown.

Training NASA astronauts in Taos:

Dr. Bill Muehlberger's familiarity with the geology of north-central New Mexico (dating back to the 1940s) served him well when he first worked with NASA during the Apollo missions of the early 1970s. His involvement began with Apollo 14. Not coincidently, Apollo 15 was the first mission to train in the Taos

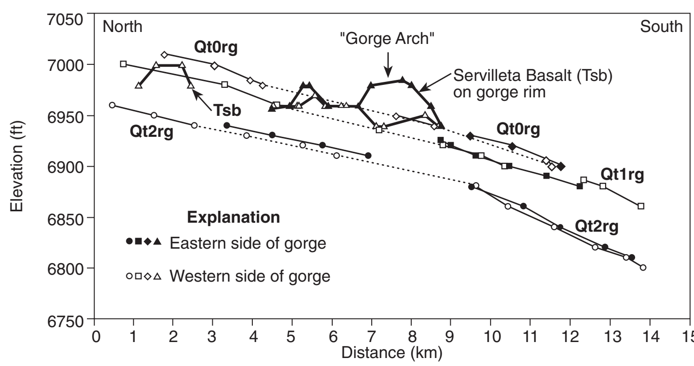

FIGURE 1.30. North-south longitudinal profiles of high Rio Grande terraces (Qt0rg, Qt1rg and Qt2rg) and Servilleta Basalt (Tsb) on the gorge rim, across the "Gorge Arch" of Muehlberger (1979). Terraces are early to middle Pleistocene in age (Kelson and Bauer, 2003), and show no deformation across the arch.

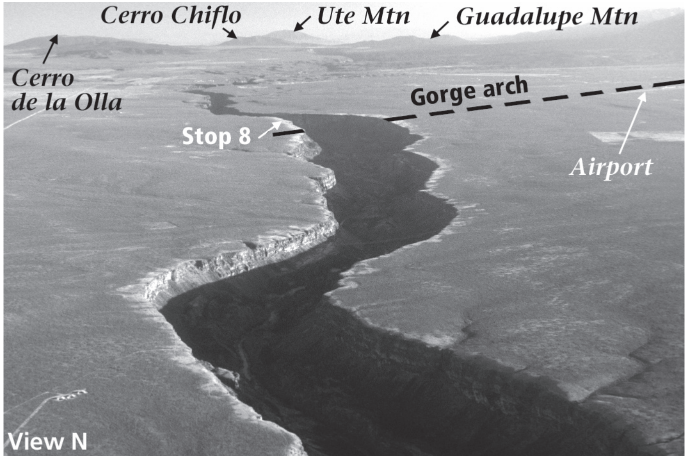

FIGURE 1.31. Aerial view north along the Rio Grande gorge showing the location of STOP 8 on the west rim. The Gorge arch trends obliquely across the photo, and corresponds with the stratigraphically highest (youngest?) basalt flow across from STOP 8, on the east rim. The Gorge arch is also coincident with the change from a narrow, steep canyon north of STOP 8, to a wide, landslide-mantled canyon to the south. Remnants of ancestral Rio Grande gravels show up as light areas along both canyon rims.

area. In March of 1971, the Apollo 15 crew trained along the east rim of the gorge, just south of here, because the gorge was a superb analogy to their lunar landing site in the Hadley Rille (Fig. 1.32). As Principal Investigator for Field Geology for the Apollo 16 and 17 missions to the Moon, Bill was responsible for training astronauts in techniques of field geology, and naturally, the Taos was again selected for field exercises. In September of 1971, Apollo 16 astronauts trained on the volcanic hills west of here, which were similar to their lunar target. The Apollo 17 crew did not visit Taos because New Mexico astronaut/geologist Jack Schmitt had already trained here. Schmitt became the first geologist to visit the Moon, and later was elected to the U.S. Senate. The northern New Mexican training exercises have continued through the Space Shuttle missions, culminating in 1999 when astronauts participated in a geophysical study of buried basin structures near the Town of Taos; this in anticipation of developing a simulation for exploring other planets such as Mars.

End of Stop 8. Return to vehicles, turn around, and retrace route back to US-64.

94.8 **Turn left, heading west. [24] 0.3**

95.9 **Turn right onto maintained gravel road. [23] 1.1**
98.7 **Turn right onto US-64. [22] 2.8**

99.3 Passing Rio Grande Gorge Rest Center on right. On left is a small remnant of the Qt2rg terrace, inset into the upper flow-package of the Servilleta Basalt. **0.6**

99.4 The Rio Grande Gorge Bridge, completed in 1965, is a beautiful engineering marvel (Fig. 1.32). It is the second longest such bridge in the country. In engineering parlance, the bridge is best termed a continuous steel deck truss, with truss spans of 300, 600 and 300 ft and a 36-ft steel I-beam approach span at each end. It is 1272 ft long with a 28-ft roadway, and was fabricated by the American Bridge Company and erected by J.H. Ryan & Son for a total cost of $2,153,000. The bridge won first place for the most beautiful span in the U.S. in 1966. The Rio Grande is 650 feet below and rafters and kayakers on the river are understandably nervous about being hit by falling debris thrown by sightseers on the bridge. For their sake, please resist the urge to study terminal velocity here. This bridge has been shown in several Hollywood movies, including *Easy Rider* (1969), *Twins* (1988), and perhaps most infamously in the wedding scene of *Natural Born Killers* (1994). Sadly, the bridge has also provided the means for several suicides and one (known) gruesome murder. **0.1**

99.7 Eastern end of gorge bridge. The surface directly east of the bridge is underlain by Qt1rg deposits, which are locally exposed in arroyo walls traversed by US-64 for about the next 2 km (1.2 mi). It is not known with confidence whether the Qt1rg deposits are inset into or interfinger with the uppermost "Blueberry Hill deposits," which are exposed in arroyo walls about 3 to 4 km from the bridge (Figs. 1.33 and 1.34; see mini-paper by Barker, p. 33). **0.3**

100.3 Ahead, we cross a series of asymmetric valleys that are within the north-tilted domain on the Hondo alluvial fan (Fig 1.2). **0.6**

FIGURE 1.32. NASA astronauts have been quietly visiting the Taos area for earth science training since the early 1970s. The southern Rio Grande gorge was especially valuable for preparation of Apollo lunar explorers such as Jim Irwin (left) and Dave Scott (shown here in 1971) due to its similarities to the lunar surface. Irwin and Scott later landed near Hadley Rille (thought to be a lava flow channel and/or a collapsed lava tube) on Apollo 15, where they performed geologic investigations of the lunar surface. They examined the only outcrop seen on any of the Apollo missions and collected 370 rock and soil samples, including a core from 2.4 m below the surface. At 1.5 km wide and 300 m deep, Hadley Rille is comparable to the Rio Grande gorge near the confluence of the Rio Pueblo de Taos and Rio Grande.

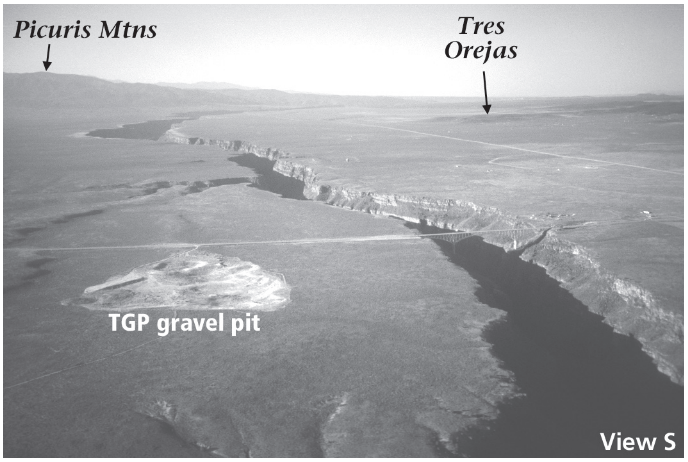

FIGURE 1.33. Aerial view southward of the Rio Grande gorge and the Gorge Bridge. The now-reclaimed, 42-acre Taos Gravel Products (TGP) quarry was developed 700 ft from the gorge rim in ancestral Rio Grande gravel (Qt1rg). The TGP operation was closed in 2002 because it was found to be too close to the Rio Grande Wild and Scenic River corridor and partially situated on un-permitted land. The Wild and Scenic Rivers Act, the nations' preeminent river protection law, is intended to protect designated free-flowing rivers from dam building, logging, mining, and cattle grazing.

103.5 Airport entrance on right. We are now on the hinge or crest of the Gorge arch, and are crossing into the domain of east-tilted stream asymmetries. **3.2**

104.9 Gravel pit on right is located on the steep flank of a well-formed, east-tilted asymmetric drainage. **1.4**

107.0 Blueberry Hill Rd. on the right. **[5]** **2.1**

107.2 Junction with NM-522 (at the stoplight formerly known as the "Blinking Light"). **[6]** **0.2**

END OF DAY 1 LOG.

ACKNOWLEDGMENTS

We appreciate a thoughtful review of the Day 1 log by William McIntosh. Brigitte Felix Kludt of Lemitar, NM, prepared many of the photos. David McCraw produced the trip route figure and Mark Mansell did the bulk of the GIS work for the Figure 1.9 and Plate 2 geologic maps.

Potential interaction of sustainable development and aggregate production with an example from Taos, New Mexico, USA

James M. Barker
New Mexico Bureau of Geology and Mineral Resources, New Mexico Institute of Mining and Technology, Socorro, New Mexico 87801

Sand and gravel or crushed stone (aggregate) production and value exceed any other mineral resource in the world and are central to our economy. Aggregate operations comprise approximately 95% of all mines, pits and quarries in the United States and approximately 75% of the newly mined resources used annually (Wagner, 2002). Per capita consumption is about 10 mt per year used primarily in fill, concrete and asphalt. Society will demand aggregate, industry will produce it, and communities near pits and quarries will complain about it—these frictions must be resolved.

Aggregate operators and local citizens have legitimate concerns, while at the same time each needs the other. This interdependency is not always recognized by citizens, but it exists and persists. Over the last quarter century or so, mechanisms to handle conflicting needs in a society have increased, mainly via sustainable development (SD). SD is a process of early proactive engagement whereby all legitimate stakeholders participate in planning an operation and in the receipt of benefits from it. Issues raised about aggregate mining in the Taos valley represent a microcosm of SD issues elsewhere and are exacerbated by the particular combination of geography, geology, and history of the valley.

Sustainable development

Sustainable development is based on a comprehensive and inclusive post-modern interaction of the social, economic and environmental systems of mankind in which interconnectedness is explicit (Langer et al., 2003). Sustainable development (SD) was defined in the Brundtland Report (United Nations, 1987) as activity that "…meets the needs of the present without compromising the ability of future generations to meet their own needs." Agenda 21 of the 1992 Earth Summit stated "Governments should adopt a national strategy for sustainable development… ." More than 300 definitions of SD exist (Anderson, 2003). The conversion of society to fully realized SD will take generations.

Intergenerational equity is a key component of all SD definitions (Barker and McLemore, 2004). Over time, human well-being must never decline under the SD paradigm. Natural, human, social, financial and manufactured capital stocks (MMSD, 2002, p. 21-23) are common measures of well being. Under a "weak" SD practice, if the total of all these capital stocks is maintained or increased for the next generation, then minimal SD has been met. Using "strong" SD practice, these capital stocks are complements, but dependencies and irreversible thresholds among them preclude unlimited substitution. Natural capital consists of both renewable resources and non-renewable resources (including aggregate) supplied by the earth, water, air, biota and environment of the planet. Human capital is the summation of people's health, knowledge, skills and motivation. Social capital consists of the institutions and relationships that help us maintain and develop human capital. Manufactured capital is composed of material goods or infrastructure that contributes to the production

FIGURE 1.34. Stockpile of ancestral Rio Grande river-gravel in a quarry on the Los Cordovas quadrangle. Most of the clasts are well-rounded Tertiary volcanic rocks.

process. Financial capital is an abstraction converted and unified from other capital stocks.

Society must grant a license to companies to produce aggregate that must reflect local conditions. An SD approach can ensure this by requiring the cooperative interaction between stakeholders in the three pillars of SD: economy, environment, and society. Government has become an indispensable fourth pillar of SD to mediate and measure success. The SD approach focuses companies on the economic value they add to society and on the environmental and social value they add or subtract from a community. A company's performance is measured against the desires of society as a whole rather than the stockholders alone. The company minimizes harm from their activities and creates net economic, social and environmental value for the non-mining segments of society. Aggregate companies that foster a society less resistant to them will gain lower operating costs (MMSD, 2002).

Legally enforced environmental cleanup, mitigation, remediation, and closure are a small part of fully engaged SD. From exploration to post closure, an aggregate company will be remembered less for what it does at closure than for what it did at start-up and during operation. At closure is too late to successfully engage stakeholders. It is not too late to further sully mining's reputation through a botched closure. Simply providing a steady stream of aggregate is not enough (Anderson, 2003). Ultimately, the aggregate company that best implements SD policies can become the company of choice for society (Yearley, 2003) and can reap the benefits of this status.

Taos, Sustainable Development and Aggregate Production

Many aggregate operations are very close to or within urban centers because this high-bulk low-value commodity is very transport sensitive. If pits are placed too far away, costs (economic and environmental) increase unnecessarily (Isaacson, 2001). If placed too close, conflict is inevitable. The image most citizens have of mining is from local aggregate operations.

The rural locale of Taos may seem to have many possible aggregate sites over a wide geographic area but such is not the case. Taos is bounded by areas of restricted land use (Fig. 1.34). The Rio Grande Wild and Scenic River area is to the west. Taos Pueblo is to the east and west; Picuris Pueblo is to the south. The Carson National Forest is east, south and west and is currently closed to aggregate development by the district ranger. The remaining land is mostly private surface based on Spanish land grants. The State and BLM have minimal surface rights; the BLM has some subsurface mineral rights in southern and northern parts of the area.

Access from the west is via the Gorge Bridge, which is the only regional major crossing of the Rio Grande and is about 18 km northwest of Taos on US-64. A very minor crossing of the river, which cannot support continuous commercial traffic, is to the south at Pilar. Major access from the south is via the narrow Canon del Rio Grande that is largely filled by the Rio Grande and a two-lane highway. Access from the north and east is over similar two-lane roads. Much of the aggregate activity in the Taos area is concentrated on both sides of the Gorge Bridge along US-64.

Aggregate resources appear to be abundant but all aggregate resources are not useable when quality and engineering specifications are considered. In Hildalgo County for instance, a region of southwestern NM with abundant surficial materials, Langer et al (1997) estimated that only 5–15% of the surficial materials

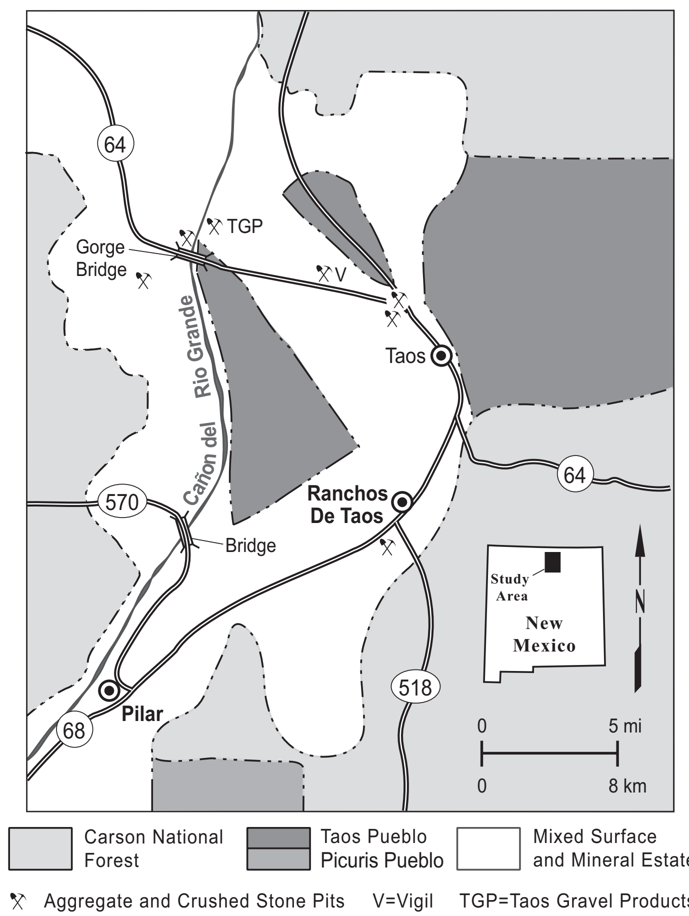

FIGURE 1.34. Basic land status and access for the Taos region showing active aggregate pits as of 2001 and the location of the TGP pit closed in 2003 (after Pfeil et al., 2001; Albuquerque Journal, 2002; McKee, 2001).

were suitable for use as aggregate. A second factor is availability, which is largely determined by urbanization. As residences spread out from a city center, large areas of aggregate are rendered unusable (sterilized) even if not built over directly (Langer, 2002).

The community of Taos has a range of choices about meeting their aggregate needs. The two clearest choices are either to accommodate nearby pits or haul aggregate from outside the immediate area. Aggregate-pit placement is difficult to gauge. If pits are placed too far away from the point of use, costs will increase unnecessarily. If pits are placed too close, once-distant pits may be engulfed by unexpected or unzoned urban growth that is exacerbated by stepping out rather than infilling. Prior rights do not always help because homeowners will knowingly purchase near an aggregate pit, then energetically lobby to have it closed. The solution to these difficult choices lies in an SD approach, which is aided by the non-toxic and low environmental impact of aggregate pits compared to most mines (Langer, 2001). This could foster a solution wherein carefully planned aggregate pits are built closer to Taos thus lowering cost and decreasing pollution. The most potent part of the SD process is bringing together all the legitimate stakeholders to reach an accord. All stakeholders have rights (even including the aggregate producers) and an expectation of equity. Joining a process that grants aggregate operators a social license to operate while mitigating the concerns of the non-mining community will benefit everyone in the Taos area.

The conflict over Taos aggregate-pit placement is exemplified by two recent legal decisions—one for and one against an aggregate producer. The Taos County Commission upheld expansion at a permitted aggregate/asphalt plant near the airport (de Bruin, 2004) against local homeowners. The housing development was started in 1991 near an existing sewage plant and gravel pits. In 2001–2002, Amigos Bravos (a non-government organization or NGO typical of those engaged in SD) won a suit against an aggregate pit near, but not in the Rio Grande Wild and Scenic River area (McKee, 2001; Albuquerque Journal, 2002) largely because the operation was erroneously placed outside the permitted area (see Figures 1.32 and 1.34).

The most likely practical solution is to curtail aggregate operations east of the Rio Grande and to foster development of aggregate pits west of the Gorge Bridge. Resources and availability are much higher there and the transport and environmental costs are manageable. The buffer supplied by the Rio Grande should lessen the potential urban growth and associated aggregate sterilization in the area west and south of the Gorge Bridge.

REFERENCES

Albuquerque Journal, 2002, Gravel mine near gorge shut: Journal North, 22 Mar 2002, p. 5.

Anderson, D., 2003, Another sustainable development 'sermon on the mount': Mining Engineering, v. 55, no. 11, p. 58–59, 63.

Barker, J. M. and McLemore, V. T., 2004, Sustainable development and industrial minerals: Society of Mining, Metallurgy and Exploration (SME), Preprint 04-171, 7 p.

de Bruin, C., 2004, Commission upholds Vigil's gravel crushing permit near Tune Drive: The Taos News, 31 Dec. 03–7 Jan. 04, p. A5.

Isaacson, A. E., 2001, Real estate development, transportation costs, and Wasatch Front gravel operations: 35th Forum on the Geology of Industrial Minerals, Utah Geological Survey, Miscellaneous Publication 01-12, p.63–71.

Langer, W. H., 2002, Managing and protecting aggregate resources: U. S. Geological Survey, OFR 02-415, 15 p.

Langer, W. H., 2001, Environmental impacts of mining natural aggregate: 35th Forum on the Geology of Industrial Minerals, Utah Geological Survey, Miscellaneous Publication 01-12, p.127–137.

Langer, W. H., Šolar, S. V., Shields, D. J., and Giusti, C., 2003, Sustainability indicators for aggregate; *in* Agioutantis, Z., ed., Proceedings, International Conference on Sustainable Development Indicators in the Mineral Industries: Milos Conference Center—George Eliopoulanos, Milos Island, p. 251–257.

Langer, W. H., Green, G. N., Bliss, J. D., and Knepper, D. H. Jr., 1997, Natural aggregate resources of the Mimbres Resource Area, southwestern New Mexico: U. S. Geological Survey, OFR 97-521, p. 463–473.

McKee, J., 2001, Taos group sues BLM over mine: Albuquerque Journal, Journal North, 6 Sept. 01, p. 4.

MMSD, 2002, Breaking new ground—mining, minerals, and sustainable development: London, Earthscan Publications, 441 p.

Pfeil, J. J., and others, 2001, Mines, mills and quarries in New Mexico: NM Bureau of Mines and Mineral Resources, State Mine Inspector, and Energy & Minerals Division, 46 p, map 1:1,000,000.

United Nations, 1987, Our Common Future, Report of the World Commission on Environment and Development [Brundtland Commission]: Oxford, Oxford University Press, 383 p.

Wagner, L. A., 2002, Materials in the Economy—Material Flows, scarcity, and the environment: U. S. Geological Survey, Circular 1221, 29 p.

Yearley, D. C., 2003, Sustainable development for the global mining and metals industry: Mining Engineering, v. 55, no. 8, August, p. 45–48.